The University of Sydney

Department of Civil Engineering
Sydney NSW 2006
AUSTRALIA

http://www.civil.usyd.edu.au/

Environmental Fluids/Wind Group

Dynamic response of a pile embedded in a porous medium subjected to plane SH waves

Research Report No R858

Frank Jian-Fei Lu, BE ME PhD
Dong-Sheng Jeng, BE ME PhD
Wei-Dong Nie, BE

December 2005

The University of Sydney

Department of Civil Engineering
Environmental Fluids/Wind Group
http://www.civil.usyd.edu.au/

Dynamic response of a pile embedded in a porous medium and subjected to plane SH waves

Research Report No R858

Frank Jian-Fei Lu, BE ME PhD
Dong-Sheng Jeng, BE ME PhD
Wei-Dong Nie, BE

December 2005

Abstract:

In this study, the frequency domain dynamic response of a pile embedded in a porous medium and subjected to SH seismic waves is investigated. The surrounding porous medium of the pile is described by Biot's theory, while the pile embedded in the porous medium is treated as a beam and described by a beam vibration theory. Using the Hankel transformation method, the fundamental solution for a half-space porous medium subjected to a horizontal circular patch load is established. According to the fictitious pile methodology, the second kind of Fredholm integral equation for the pile is established in terms of the obtained fundamental solution and free wave field. The solution of the integral equation yields the dynamic response of the pile to plane SH waves. Numerical results indicate that the parameters of the porous medium, the pile and the incident wave have considerable influences on the dynamic response of the pile and the porous medium.

Keywords:

Biot's theory; pile; SH waves; Fredholm integral equation; porous media.

Copyright Notice

Department of Civil Engineering, Research Report R858
Dynamic response of a pile embedded in a porous medium and subjected to plane SH waves

f.lu@civil.usyd.edu.au d.jeng@civil.usyd.edu.au

Published by:
Department of Civil Engineering
The University of Sydney
Sydney NSW 2006
AUSTRALIA

December 2005

This report and other Research Reports published by The Department of Civil Engineering are available on the Internet:

http://www.civil.usyd.edu.au

Contents

1. Introduction[1]

Pile foundations have been commonly used when the strength of soil base is insufficient to support the load from the superstructures. To make the static force or settlement experienced by the pile foundation satisfy practical requirements, various approaches have been developed for static pile foundation design (Broms, 1964; Muki and Sternberg, 1970; Butterfield and Banerjel, 1971; Poulos and Davis, 1980;). Besides static loads from superstructures, the dynamic load due to seismic waves is also a key factor to take into account when performing pile foundation design. In some cases, seismic waves can generate dramatic damage to pile foundations (Youd and Bartlett, 1964; Karkee and Kishida, 1997). Consequently, the calculation of the dynamic response of pile foundations to seismic waves is crucial for earthquake and civil engineering.

To date, several methodologies have been proposed to calculate the dynamic response of pile foundations subjected to seismic waves (Takemiya and Yamada, 1981; Sen et al., 1985; Mamoon and Banerjee, 1990; Fan et al., 1991). Both continuum and Winkler-type models have been used to investigate the dynamic response of pile foundations to seismic waves. However, existing models for the dynamic analysis of pile foundations subjected to seismic waves have been limited to the single phase case, i.e., the surrounding media of the pile foundations are treated as single phase media. In fact, some pile foundations are embedded in saturated porous media, for example, saturated soil or saturated rock. Obviously, the single phase model is not appropriate for the design of pile foundations embedded in saturated porous media. The main drawback of the single phase model lies in that it can not predict the influence of permeability of porous media on the dynamic response of pile foundations. Also, evaluation of pore pressure increment during the passage of seismic waves is beyond the applicability of the single phase model. However, pore pressure near pile foundation due to seismic waves is crucial for understanding and exploring mechanisms of the liquefaction of the soil surrounding pile foundations. Experimental and analytical analyses show that pore pressure increment near pile foundations due to seismic waves plays a significant role in the liquefaction of the soil surrounding pile foundations (Berill and Yasuda, 2002; Tokimatsu and Suzuki, 2004). To the best of the authors' knowledge, existing investigations concerning the dynamic response of the pile foundation embedded in porous media are essentially restricted to pile foundations subjected to a harmonic top load (Zeng and Rajapakse, 1999; Lu, 2002;

[1] This report is part of the manuscript:: Lu, J.-F., Jeng, D.-S. and Nie, W-D. (2005): Dynamic response of a pile embedded in a porous medium and subjected to plane SH waves. *Computers and Geotechnics* (submitted)

Wang et al., 2003). For dynamic response of a pile foundation embedded in porous media to seismic waves, no research has been carried out so far.

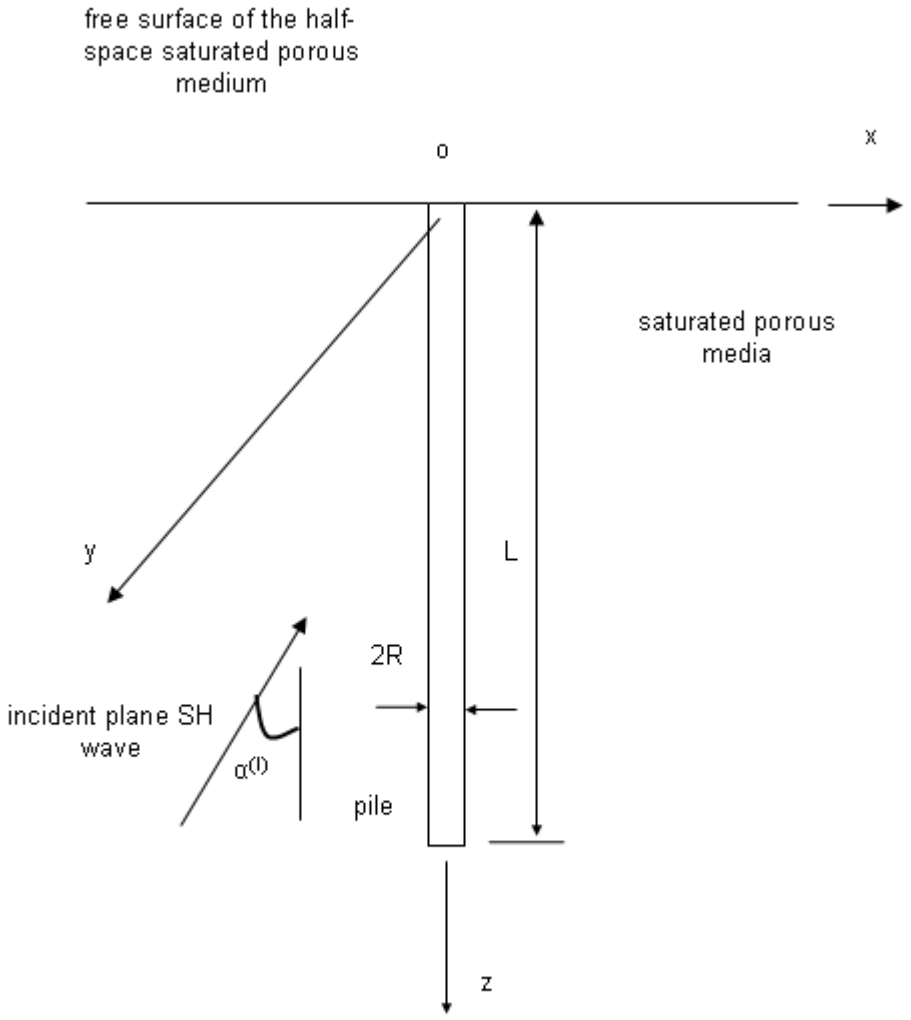

Figure 1: A pile embedded in a half-space porous medium and subjected to a plane SH wave

The aim of this study is to investigate the frequency domain dynamic response of a pile embedded in a porous medium subjected to plane SH seismic waves (Figure 1). The saturated porous medium surrounding the pile is described by Biot's poro-elastic theory[16-19], while the pile embedded in the porous medium is treated as a beam and described by a beam vibration theory. By using the Fourier transformation method and introducing two

scalar potentials and one vector potential for the porous medium, the governing equations for Biot's theory are reduced to three Helmholtz equations. Using the Hankel transformation method, the fundamental solution for a half-space porous medium subjected to a horizontal circular uniform patch load is established. According to the fictitious pile methodology, the current pile-soil interaction problem is decomposed into a extended half-space porous medium and a fictitious pile (Muki and Stemberg, 1970). The rotary angle of the pile axis and the extended half space at z-axis is used to construct the compatibility condition between the pile and the half space. The second kind of Fredholm integral equation for the pile subjected to SH waves is constructed in terms of the obtained fundamental solution and the compatibility condition between the half-space and the fictitious pile. Numerical solution of the integral equation yields the dynamic response of the pile to the traveling SH wave. A parametric study for the dynamic response of the pile in porous medium is performed.

2. Theoretical Formulations

2.1 Governing equations for porous media

In this study, the porous medium surrounding the pile is described by Biot's theory (Biot, 1941; 1956a, b; 1962). The constitutive equations for homogeneous porous medium can be expressed as (Biot, 1941; 1956a, b; 1962)

$$\sigma_{ij} = 2\mu\varepsilon_{ij} + \lambda\delta_{ij}e - \alpha\delta_{ij}p\,, \tag{1a}$$

$$p = -\alpha Me + M\vartheta\,, \tag{1b}$$

$$e = u_{i,i}\,, \tag{1c}$$

$$\vartheta = -w_{i,i}\,, \tag{1d}$$

where u_i and w_i denote the average solid displacement and the fluid displacement relative to the solid frame; ε_{ij} and e are the strain tensor and the dilatation of the solid skeleton; ϑ is the fluid volume variation of a unit reference porous medium; σ_{ij} is the stress of bulk material; p is the excess pore fluid pressure and δ_{ij} is the Kronecker delta, λ and μ are Lame constants of the solid skeleton; α and M are Biot parameters (Biot, 1941) accounting for the compressibility of the saturated porous medium. Note that $0 \le \alpha \le 1, 0 \le M < \infty$, and $M \to 0$ for completely dry materials, while $\alpha \to 1, M \to \infty$ for materials with

incompressible constituents. The expression for the fluid discharge in *i*-th ($i = x, y, z$) direction has the following form

$$q_i = \frac{\partial w_i}{\partial t}. \tag{2}$$

The equation of motion for the bulk material and the pore fluid are expressed in terms of the displacements u_i and w_i

$$\mu u_{i,jj} + (\lambda + \mu) u_{j,ji} - \alpha p_i = \rho_b \ddot{u}_i + \rho_f \ddot{w}_i, \tag{3a}$$

$$-p_i = \rho_f \ddot{u}_i + m\ddot{w}_i + \frac{\eta}{k} K(t) * \dot{w}_i, \tag{3b}$$

where ρ_b, ρ_f denote the bulk density of the porous medium and the density of the pore fluid, $\rho_b = (1-\phi)\rho_s + \phi\rho_f$, ρ_s is the density of the solid skeleton and ϕ is the porosity of the porous medium; $m = a_\infty \rho_f / \phi$ and a_∞ is tortuosity; η and k represent the viscosity of the pore fluid and the permeability of the porous medium, respectively and $K(t)$ is a time dependent viscosity correction factor which describes the transition behavior from viscosity dominated flow in the low frequency range towards inertia dominated flow at high frequency range (Biot, 1956a, Johnson et al., 1987; Pride et al., 1993); a superimposed dot on a variable denotes the derivative with respect to time and a star between two variables denotes time convolution.

When deriving the general solutions for Biot's equations, the Fourier transformation with respect to time and frequency are involved. In this paper, the Fourier transformation for time and frequency is defined as follows (Sneddon, 1951)

$$\hat{f}(\omega) = \int_{-\infty}^{+\infty} f(t) e^{-i\omega t} dt, \tag{4a}$$

$$f(t) = \frac{1}{2\pi} \int_{-\infty}^{+\infty} \hat{f}(\omega) e^{i\omega t} d\omega, \tag{4b}$$

where t and ω denote time and frequency, respectively.

To eliminate time derivatives in (1)-(3), the Fourier transformation with respect to time is performed on (1)-(3). As a result, all the governing equations are transformed into the

frequency domain. Accordingly, the following derivations will be developed in the frequency domain.

In terms of the Helmholtz decomposition method, in Cartesian coordinate system, the solid displacement has the following decomposition

$$\hat{u}_i = \hat{\varphi}_{,i} + e_{ijk}\hat{\psi}_{k,j}, \tag{5}$$

where a caret denotes the Fourier transformation with respect to time, $\hat{\varphi}$ and $\hat{\psi}_k$ ($k = 1,2,3$) are the scalar and vector potential for the porous medium and e_{ijk} is the Levi-Civita symbol. Moreover, in the Cartesian coordinate system, the vector potential $\hat{\psi}_k$ ($k = 1,2,3$) satisfies the following gauge condition

$$\hat{\psi}_{i,i} = 0 . \tag{6}$$

Since two kinds of *P* waves (P_1 wave and P_2 wave) exist in the porous medium, the displacement in (5) can be further represented by (Zimmeman and Stern, 1993)

$$\hat{u}_i = \hat{\varphi}_{,i} + e_{ijk}\hat{\psi}_{k,j} = \hat{\varphi}_{f,i} + \hat{\varphi}_{s,i} + e_{ijk}\hat{\psi}_{k,j}, \tag{7}$$

where $\hat{\varphi}_f$ and $\hat{\varphi}_s$ denote scalar potentials corresponding to P_1 wave and P_2 wave, respectively.

According to the analysis of Bonnet (Bonnet, 1987), although two displacement vectors are used in Biot's theory, four independent variables exist in a two-phase porous medium. Consequently, the pore pressure has the following expression

$$\hat{p} = A_f\hat{\varphi}_{f,ii} + A_s\hat{\varphi}_{s,ii}, \tag{8}$$

where A_f and A_s are two constants to be determined by the governing equations of Biot's theory.

Using the frequency domain expressions of (1b), (3b) and (7), (8) as well as (3a), we have

$$[(\lambda + 2\mu - \beta_2 A_f)\hat{\varphi}_{f,jj} + \beta_3\ \hat{\varphi}_f]_{,i} + [(\lambda + 2\mu - \beta_2 A_s)\hat{\varphi}_{s,jj} + \beta_3\ \hat{\varphi}_s]_{,i}$$

$$+ e_{iml}[\mu\hat{\psi}_{l,jj} + \beta_3\ \hat{\psi}_l]_{,m} = 0, \tag{9}$$

where $\beta_3 = \rho\omega^2 - {\rho_f}^2\omega^4 / \beta_1$, $\beta_2 = \alpha - \rho_f\ \omega^2 / \beta_1$, $\beta_1 = m\omega^2 - i\eta\omega\hat{K}(\omega)/k$. Fulfillment of (9) requires each expression in the square braces of (9) vanishes independently, which leads to

$$(\lambda + 2\mu - \beta_2 A_f)\hat{\varphi}_{f,jj} + \beta_3\ \hat{\varphi}_f = 0, \tag{10a}$$

$$(\lambda + 2\mu - \beta_2 A_s)\hat{\varphi}_{s,jj} + \beta_3\ \hat{\varphi}_s = 0, \tag{10b}$$

$$\mu\hat{\psi}_{i,jj} + \beta_3\hat{\psi}_i = 0. \tag{10c}$$

Similarly, using equation (1b), (1c), (1d) and (3b), one has

$$\hat{p}_{,ii} + \frac{\beta_1}{M}\hat{p} + (\alpha\beta_1 - \rho_f\omega^2)\hat{u}_{i,i} = 0, \tag{11}$$

then, substitution of (7) and (8) into (11) leads to

$$[A_f\hat{\varphi}_{f,ii} + (\beta_5 A_f - \beta_4)\hat{\varphi}_f]_{,jj} + [A_s\hat{\varphi}_{s,ii} + (\beta_5 A_s - \beta_4)\hat{\varphi}_s]_{,jj} = 0. \tag{12}$$

Again, fulfillment of the above equation leads to the following expressions

$$A_f\hat{\varphi}_{f,ii} + (\beta_5 A_f - \beta_4)\hat{\varphi}_f = 0, \tag{13a}$$

$$A_s\hat{\varphi}_{s,ii} + (\beta_5 A_s - \beta_4)\hat{\varphi}_s = 0, \tag{13b}$$

where $\beta_4 = \rho_f\omega^2 - \alpha\beta_1$, $\beta_5 = \beta_1 / M$.

Using (10a), (10b), (13a) and (13b), we have

$${A_{f,s}}^2 + \frac{\beta_3 - (\lambda + 2\mu)\beta_5 - \beta_2\beta_4}{\beta_2\beta_5}A_{f,s} + \frac{(\lambda + 2\mu)\beta_4}{\beta_2\beta_5} = 0, \tag{14}$$

from which, the values of A_f, A_s can be determined.

Equations (10) and (13) can be reduced to Helmholtz equations by introducing the following quantities,

$${k_f}^2 = \frac{\beta_3}{\lambda + 2\mu - \beta_2 A_f} = \frac{\beta_5 A_f - \beta_4}{A_f}, \tag{15a}$$

$$k_s^{\,2} = \frac{\beta_3}{\lambda + 2\mu - \beta_2 A_s} = \frac{\beta_5 A_s - \beta_4}{A_s}, \tag{15b}$$

$$k_t^{\,2} = \frac{\beta_3}{\mu}, \tag{15c}$$

which have the form

$$\nabla^2 \hat{\varphi}_f + k_f^{\,2} \hat{\varphi}_f = 0 \tag{16a}$$

$$\nabla^2 \hat{\varphi}_s + k_s^{\,2} \hat{\varphi}_s = 0 \tag{16b}$$

$$\nabla^2 \hat{\boldsymbol{\psi}} + k_t^{\,2} \hat{\boldsymbol{\psi}} = 0 \tag{16c}$$

where k_f, k_s, k_t are the complex wave number for the P_1, P_2 and S wave of the porous medium. To guarantee the attenuation of the body waves, $\mathrm{Im}(k_f), \mathrm{Im}(k_s), \mathrm{Im}(k_t)$ should be non-positive. Also, since the speed of the P1 wave is larger than that of the P2 wave, as a result, the inequality $\mathrm{Re}(k_f) \le \mathrm{Re}(k_s)$ should always hold.

Equation (16) determines the three potentials for the porous medium. After determining the potentials for the porous medium, the frequency domain displacements, stresses and pore pressure are given by (7), (1) and (8). The relative displacement between the solid skeleton and pore fluid can be derived by (3b) and has the following form

$$\hat{w}_i = \frac{1}{\beta_1} \hat{p}_{,i} - \frac{\rho_f \omega^2}{\beta_1} \hat{u}_i \tag{17}$$

2.2 Fundamental solution for a half-space porous medium subjected to a horizontal circular patch load

In Section 2.1, the governing equations for Biot's theory have been reduced to Helmholtz equations for two scalar potentials and one vector potential [i.e., (16)]. In this section, the fundamental solution for a half-space porous medium subjected to a uniform horizontal patch load over a circular domain with radius R (see Figure 2) will be established. The resultant of the patch load is assumed to be unity. Since the half space considered here is a symmetric configuration, it is more convenient to consider our problem in a cylindrical coordinate system (r, θ, z). In the cylindrical coordinate system, the vector potential $\hat{\boldsymbol{\psi}}$ for the solid

skeleton and pore fluid displacements can be reduced to two scalar potentials $\hat{\chi}$ and $\hat{\eta}$ (Achenbach, 1973). The potentials, $\hat{\varphi}_f$, $\hat{\varphi}_s$, $\hat{\chi}$ and $\hat{\eta}$, therefore, satisfy the following Helmholtz equations in the cylindrical coordinate system (r,θ,z)

$$(\frac{\partial^2}{\partial r^2}+\frac{1}{r}\frac{\partial}{\partial r}+\frac{1}{r^2}\frac{\partial^2}{\partial \theta^2}+\frac{\partial^2}{\partial z^2})\hat{\varphi}_f+k_f^2\hat{\varphi}_f=0, \tag{18a}$$

$$(\frac{\partial^2}{\partial r^2}+\frac{1}{r}\frac{\partial}{\partial r}+\frac{1}{r^2}\frac{\partial^2}{\partial \theta^2}+\frac{\partial^2}{\partial z^2})\hat{\varphi}_s+k_s^2\hat{\varphi}_s=0, \tag{18b}$$

$$(\frac{\partial^2}{\partial r^2}+\frac{1}{r}\frac{\partial}{\partial r}+\frac{1}{r^2}\frac{\partial^2}{\partial \theta^2}+\frac{\partial^2}{\partial z^2})\hat{\chi}+k_t^2\hat{\chi}=0, \tag{18c}$$

$$(\frac{\partial^2}{\partial r^2}+\frac{1}{r}\frac{\partial}{\partial r}+\frac{1}{r^2}\frac{\partial^2}{\partial \theta^2}+\frac{\partial^2}{\partial z^2})\hat{\eta}+k_t^2\hat{\eta}=0 \tag{18d}$$

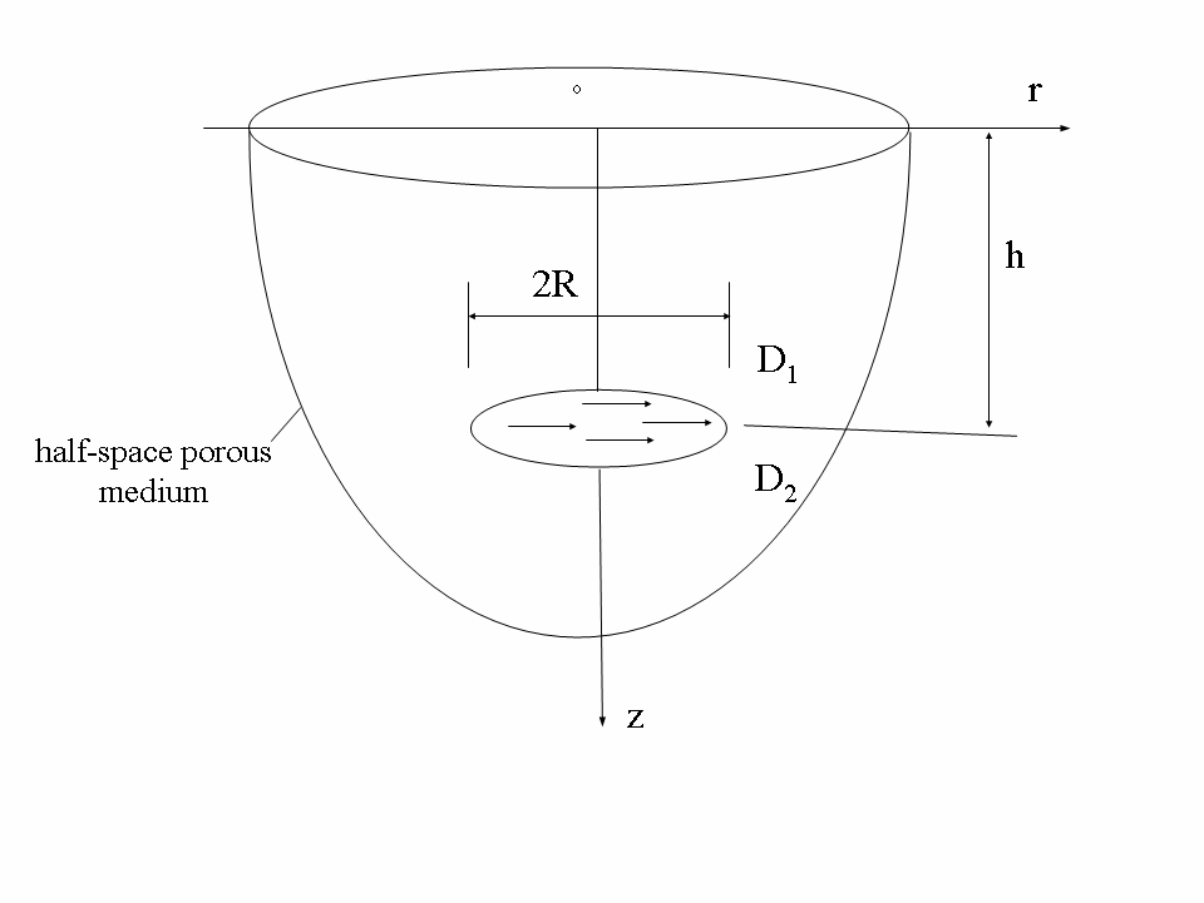

Figure 2 Horizontal uniform circular patch load applied inside a poroelastic half-space.

The displacements can be expressed in terms of the potentials in cylindrical coordinate system (r,θ,z) as

$$\hat{u}_r = \frac{\partial \hat{\varphi}_f}{\partial r} + \frac{\partial \hat{\varphi}_s}{\partial r} + \frac{1}{r}\frac{\partial \hat{\chi}}{\partial \theta} + \frac{\partial^2 \hat{\eta}}{\partial r \partial z}, \tag{19a}$$

$$\hat{u}_\theta = \frac{1}{r}\frac{\partial \hat{\varphi}_f}{\partial \theta} + \frac{1}{r}\frac{\partial \hat{\varphi}_s}{\partial \theta} - \frac{\partial \hat{\chi}}{\partial r} + \frac{1}{r}\frac{\partial^2 \hat{\eta}}{\partial \theta \partial z}, \tag{19b}$$

$$\hat{u}_z = \frac{\partial \hat{\varphi}_f}{\partial z} + \frac{\partial \hat{\varphi}_s}{\partial z} - \frac{1}{r}\frac{\partial}{\partial r}\left(r\frac{\partial \hat{\eta}}{\partial r}\right) - \frac{1}{r^2}\frac{\partial^2 \hat{\eta}}{\partial \theta^2}), \tag{19c}$$

$$\hat{w}_r = \frac{1}{\beta_1}\frac{\partial \hat{p}}{\partial r} - \frac{\rho_f \omega^2}{\beta_1}\hat{u}_r, \tag{19d}$$

$$\hat{w}_\theta = \frac{1}{\beta_1 r}\frac{\partial \hat{p}}{\partial \theta} - \frac{\rho_f \omega^2}{\beta_1}\hat{u}_\theta, \tag{19e}$$

$$\hat{w}_z = \frac{1}{\beta_1}\frac{\partial \hat{p}}{\partial z} - \frac{\rho_f \omega^2}{\beta_1}\hat{u}_z. \tag{19f}$$

Note that the pore pressure is given by Equation (8), while the stresses of the porous medium are determined via Equation (1a) using the expressions of the displacements as well as the pore pressure.

For an arbitrary force applied at the interior of a half-space porous medium, the potentials, displacements and stresses as well as the pore pressure can be expanded into the following series form (Muki, 1960)

$$\hat{\varphi}_f(r,\theta,z,\omega) = \sum_{m=0}^{\infty} \hat{\varphi}_{fm}(r,z,\omega)\cos(m\theta), \tag{20a}$$

$$\hat{\varphi}_s(r,\theta,z,\omega) = \sum_{m=0}^{\infty} \hat{\varphi}_{sm}(r,z,\omega)\cos(m\theta), \tag{20b}$$

$$\hat{\eta}(r,\theta,z,\omega) = \sum_{m=0}^{\infty} \hat{\eta}_{m}(r,z,\omega)\cos(m\theta), \tag{20c}$$

$$\hat{\chi}(r,\theta,z,\omega) = \sum_{m=0}^{\infty} \hat{\chi}_{m}(r,z,\omega)\sin(m\theta), \tag{20d}$$

$$\hat{u}_r(r,\theta,z,\omega)=\sum_{m=0}^{\infty}\hat{u}_{rm}(r,z,\omega)\cos(m\theta)\,, \tag{21a}$$

$$\hat{u}_\theta(r,\theta,z,\omega)=\sum_{m=0}^{\infty}\hat{u}_{\theta m}(r,z,\omega)\sin(m\theta)\,, \tag{21b}$$

$$\hat{u}_z(r,\theta,z,\omega)=\sum_{m=0}^{\infty}\hat{u}_{zm}(r,z,\omega)\cos(m\theta)\,, \tag{21c}$$

$$\hat{p}(r,\theta,z,\omega)=\sum_{m=0}^{\infty}\hat{p}_{m}(r,z,\omega)\cos(m\theta)\,, \tag{22}$$

$$\hat{\sigma}_{zz}(r,\theta,z,\omega)=\sum_{m=0}^{\infty}\hat{\sigma}_{zzm}(r,z,\omega)\cos(m\theta)\,, \tag{23a}$$

$$\hat{\sigma}_{zr}(r,\theta,z,\omega)=\sum_{m=0}^{\infty}\hat{\sigma}_{zrm}(r,z,\omega)\cos(m\theta)\,, \tag{23b}$$

$$\hat{\sigma}_{z\theta}(r,\theta,z,\omega)=\sum_{m=0}^{\infty}\hat{\sigma}_{z\theta m}(r,z,\omega)\sin(m\theta)\,, \tag{23c}$$

$$\hat{\sigma}_{rr}(r,\theta,z,\omega)=\sum_{m=1}^{\infty}\hat{\sigma}_{rrm}(r,z,\omega)\cos(m\theta)\,, \tag{23d}$$

$$\hat{\sigma}_{\theta\theta}(r,\theta,z,\omega)=\sum_{m=0}^{\infty}\hat{\sigma}_{\theta\theta m}(r,z,\omega)\cos(m\theta) \tag{23e}$$

where subscript *m* denotes the order of the term in the series.

When deriving general solutions for the porous medium in the cylindrical coordinate system (r,θ,z), the Hankel integral transformation is employed. The *m*-th order Hankel transformation is defined as follows (Sneddon, 1951)

$$\bar{f}^{(m)}(\zeta)=\int_0^{+\infty} rf(r)J_m(\zeta r)dr\,, \tag{24a}$$

$$f(r)=\int_0^{+\infty}\zeta\ \bar{f}^{(m)}(\zeta)J_m(\zeta r)d\zeta\,, \tag{24b}$$

where $J_m(\bullet)$ denotes the *m*-th order first kind of Bessel function and a bar above a variable denotes the Hankel transformation.

Substituting *m*-th component of the potentials $\hat{\varphi}_f$, $\hat{\varphi}_s$, $\hat{\eta}$, $\hat{\chi}$ in equation (20) into (18) and performing *m*-th order Hankel transformation with respect to radial coordinate *r* on the resulting equations, the following expressions for the potential components $\tilde{\varphi}_{fm}$, $\tilde{\varphi}_{sm}$, $\tilde{\eta}_m$, $\tilde{\chi}_m$ in the frequency-wave number domain are obtained

$$\tilde{\varphi}_{fm}^{(m)} = \overline{\hat{\varphi}}_{fm}^{(m)}(\xi, z, \omega) = A_m(\xi,\omega)e^{\gamma_f z} + B_m(\xi,\omega)e^{-\gamma_f z}, \tag{25a}$$

$$\tilde{\varphi}_{sm}^{(m)} = \overline{\hat{\varphi}}_{sm}^{(m)}(\xi, z, \omega) = C_m(\xi,\omega)e^{\gamma_s z} + D_m(\xi,\omega)e^{-\gamma_s z}, \tag{25b}$$

$$\tilde{\chi}_m^{(m)} = \overline{\hat{\chi}}_m^{(m)}(\xi, z, \omega) = E_m(\xi,\omega)e^{\gamma_s z} + F_m(\xi,\omega)e^{-\gamma_s z}, \tag{25c}$$

$$\tilde{\eta}_m^{(m)} = \overline{\hat{\eta}}_m^{(m)}(\xi, z, \omega) = G_m(\xi,\omega)e^{\gamma_s z} + H_m(\xi,\omega)e^{-\gamma_s z}, \tag{25d}$$

where a tilde represents the combination of the Fourier transformation and the Hankel transformation, while the superscript *m* denotes the *m*-th order Hankel transformation. In (25), ξ denotes the horizontal wave number, $\gamma_f = \sqrt{\xi^2 - k_f^2}$, $\gamma_s = \sqrt{\xi^2 - k_s^2}$, $\gamma_t = \sqrt{\xi^2 - k_t^2}$ and $A_m(\xi,\omega)$, $B_m(\xi,\omega)$, $C_m(\xi,\omega)$, $D_m(\xi,\omega)$, $E_m(\xi,\omega)$, $F_m(\xi,\omega)$, $G_m(\xi,\omega)$, $H_m(\xi,\omega)$ are arbitrary constants to be determined by the boundary conditions and continuity conditions at the horizontal plane passing through the patch load. Note that the real part of $\gamma_\alpha, \alpha = f, s, t$ in (25) should be always non-negative.

Similarly, applying the Hankel transformation to equations (19) and (21)-(23), the *m*-th component displacements, stresses and the pore pressure in the frequency wave-number domain may be expressed as follows

$$\tilde{u}_{rm}^{(m+1)} + \tilde{u}_{\theta m}^{(m+1)} = -\xi\tilde{\varphi}_{fm}^{(m)} - \xi\tilde{\varphi}_{sm}^{(m)} + \xi\tilde{\chi}_m^{(m)} - \xi\frac{d\tilde{\eta}_m^{(m)}}{dz}, \tag{26a}$$

$$\tilde{u}_{rm}^{(m-1)} - \tilde{u}_{\theta m}^{(m-1)} = \xi\tilde{\varphi}_{fm}^{(m)} + \xi\tilde{\varphi}_{sm}^{(m)} + \xi\tilde{\chi}_m^{(m)} + \xi\frac{d\tilde{\eta}_m^{(m)}}{dz}, \tag{26b}$$

$$\tilde{u}_{zm}^{(m)} = \frac{d\tilde{\varphi}_{fm}^{(m)}}{dz} + \frac{d\tilde{\varphi}_{sm}^{(m)}}{dz} + \xi^2\tilde{\eta}_{sm}^{(m)}, \tag{26c}$$

$$\tilde{p}_m^{(m)} = -A_f k_f^2 \tilde{\varphi}_{fm}^{(m)} - A_s k_s^2 \tilde{\varphi}_{sm}^{(m)}, \tag{26d}$$

$$\tilde{\sigma}_{zzm}^{(m)} = 2\mu \frac{d\tilde{u}_{zm}^{(m)}}{dz} + \lambda[(\frac{d^2\tilde{\varphi}_{fm}^{(m)}}{dz^2} - \xi^2\tilde{\varphi}_{fm}^{(m)}) + (\frac{d^2\tilde{\varphi}_{sm}^{(m)}}{dz^2} - \xi^2\tilde{\varphi}_{sm}^{(m)})] - \alpha\tilde{p}_m^{(m)}, \quad (26e)$$

$$\tilde{\sigma}_{zrm}^{(m+1)} + \tilde{\sigma}_{z\theta m}^{(m+1)} = \mu(\frac{d\tilde{u}_{rm}^{(m+1)}}{dz} + \frac{d\tilde{u}_{\theta m}^{(m+1)}}{dz}) - \mu\xi\tilde{u}_{zm}^{(m)}, \quad (26f)$$

$$\tilde{\sigma}_{zrm}^{(m-1)} - \tilde{\sigma}_{z\theta m}^{(m-1)} = \mu(\frac{d\tilde{u}_{rm}^{(m-1)}}{dz} - \frac{d\tilde{u}_{\theta m}^{(m-1)}}{dz}) + \mu\xi\tilde{u}_{zm}^{(m)}, \quad (26g)$$

$$\tilde{\Sigma}_{rrm}^{(m)} = \mu\xi(\tilde{u}_{rm}^{(m+1)} + \tilde{u}_{\theta m}^{(m+1)}) - \mu\xi(\tilde{u}_{rm}^{(m-1)} - \tilde{u}_{\theta m}^{(m-1)}) + \lambda[(\frac{d^2\tilde{\varphi}_{sm}^{(m)}}{dz^2} - \xi^2\tilde{\varphi}_{sm}^{(m)})$$

$$+ (\frac{d^2\tilde{\varphi}_{sm}^{(m)}}{dz^2} - \xi^2\tilde{\varphi}_{sm}^{(m)})] - \alpha\tilde{p}_m^{(m)}, \quad (26h)$$

$$\tilde{\Sigma}_{r\theta m}^{(m)} = \frac{1}{2}\mu\xi[(\tilde{u}_{rm}^{(m+1)} + \tilde{u}_{\theta m}^{(m+1)}) + (\tilde{u}_{rm}^{(m-1)} - \tilde{u}_{\theta m}^{(m-1)})], \quad (26i)$$

$$\tilde{\Sigma}_{\theta\theta m}^{(m)} = \lambda[(\frac{d^2\tilde{\varphi}_{fm}^{(m)}}{dz^2} - \xi^2\tilde{\varphi}_{fm}^{(m)}) + (\frac{d^2\tilde{\varphi}_{fm}^{(m)}}{dz^2} - \xi^2\tilde{\varphi}_{fm}^{(m)})] - \alpha\tilde{p}_m^{(m)} \quad (26j)$$

where superscripts m , $m+1$ and $m-1$ denote the Hankel transformation order and

$\hat{\Sigma}_{rr\,m} = \hat{\sigma}_{rr\,m} + 2\mu(\hat{u}_{rm}/r + m\hat{u}_{\theta m}/r)$, $\hat{\Sigma}_{\theta\theta\,m} = \hat{\sigma}_{\theta\theta\,m} - 2\mu(\hat{u}_{rm}/r + m\hat{u}_{\theta m}/r)$,

$\hat{\Sigma}_{r\theta n} = \hat{\sigma}_{r\theta m} + 2\mu(\hat{u}_{\theta n}/r + m\hat{u}_{rm}/r)$.

It is noted that for the fundamental solution of a half-space subjected to a horizontal patch load, the corresponding solution only involves one term in the series solutions (20)-(23): it only contains $m = 1$ term and all the other terms vanish. For the problem in Figure 2, along the horizontal plane of the circular patch load, the porous half space is divided into two domains: D1 and D2. At the surface of the D1, appropriate boundary conditions should be imposed. At the interface between D1 and D2, corresponding continuity conditions should be satisfied by the solutions in D1 and D2 domain.

The following boundary conditions hold at the surface of D1,

$\tilde{\sigma}_{zz1}^{(1)}(\xi,0,\omega) = 0$, $\tilde{\sigma}_{zr1}^{(2)}(\xi,0,\omega) + \tilde{\sigma}_{z\theta 1}^{(2)}(\xi,0,\omega) = 0$, $\tilde{\sigma}_{zr1}^{(0)}(\xi,0,\omega) - \tilde{\sigma}_{z\theta 1}^{(0)}(\xi,0,\omega) = 0$,

$\tilde{p}_1^{(1)}(\xi,0,\omega) = 0$ (permeable surface), $\tilde{w}_{z1}^{(1)}(\xi,0,\omega) = 0$ (impermeable surface) (27)

At the horizontal plane passing through the circular uniform patch load, the continuity conditions have the following form

$$\widetilde{u}_{r1}^{(2)}(\xi,h^-,\omega)+\widetilde{u}_{\theta 1}^{(2)}(\xi,h^-,\omega)=\widetilde{u}_{r1}^{(2)}(\xi,h^+,\omega)+\widetilde{u}_{\theta 1}^{(2)}(\xi,h^+,\omega),$$

$$\widetilde{u}_{r1}^{(0)}(\xi,h^-,\omega)-\widetilde{u}_{\theta 1}^{(0)}(\xi,h^-,\omega)=\widetilde{u}_{r1}^{(0)}(\xi,h^+,\omega)-\widetilde{u}_{\theta 1}^{(0)}(\xi,h^+,\omega),$$

$$\widetilde{u}_{z1}^{(1)}(\xi,h^-,\omega)=\widetilde{u}_{z1}^{(1)}(\xi,h^+,\omega),\ \widetilde{w}_{z1}^{(1)}(\xi,h^-,\omega)=\widetilde{w}_{z1}^{(1)}(\xi,h^+,\omega),$$

$$\widetilde{p}_{1}^{(1)}(\xi,h^-,\omega)=\widetilde{p}_{1}^{(1)}(\xi,h^+,\omega),\ \widetilde{\sigma}_{zz1}^{(1)}(\xi,h^-,\omega)=\widetilde{\sigma}_{zz1}^{(1)}(\xi,h^+,\omega),$$

$$\widetilde{\sigma}_{zr1}^{(2)}(\xi,h^-,\omega)+\widetilde{\sigma}_{z\theta 1}^{(2)}(\xi,h^-,\omega)=\widetilde{\sigma}_{zr1}^{(2)}(\xi,h^+,\omega)+\widetilde{\sigma}_{z\theta 1}^{(2)}(\xi,h^+,\omega),$$

$$[\widetilde{\sigma}_{zr1}^{(0)}(\xi,h^+,\omega)-\widetilde{\sigma}_{z\theta 1}^{(0)}(\xi,h^+,\omega)]-[\widetilde{\sigma}_{zr1}^{(0)}(\xi,h^-,\omega)-\widetilde{\sigma}_{z\theta 1}^{(0)}(\xi,h^-,\omega)]=-\frac{2J_1(R\xi)}{\pi R\,\xi} \qquad (28)$$

where arguments h^- and h^+ of the above variables imply the related variables tend to the load plane from the D1 and D2 domain, respectively. The general solutions for the potentials in the domains D1 and D2 are given by equation (25). It is noted that eight arbitrary constants are involved in the D1 domain. However, to guarantee the bounded solutions in the D2 domain, the positive exponential terms should vanish. Consequently, only four arbitrary constants are involved. In terms of the expressions of the potentials, the expressions for the displacements, stresses as well as pore pressure can be calculated in a straightforward way using (26). Using the expressions for the displacements, stresses as well as pore pressure, the twelve unknown constants for the D1 and D2 domain can be calculated by twelve linear algebraic equations (27) and (28).

After determination of twelve unknown constants by (27), (28), the expression for the displacements, stresses and pore pressure in the frequency wave-number domain are available. In this study, we are only concerned with the frequency domain solution. It follows from (24) that the frequency domain solution can be obtained by performing inverse Hankel transformation on the frequency wave-number domain solution. Note that due to the drag force between the solid skeleton and pore fluid, the porous medium described by Biot's theory is dissipative. Consequently, the Raleigh wave equation involved in expressions of displacements, stresses and pore pressure of the porous medium only has complex roots. Thus, the integration axis-ξ is free of any singularity and consequently the inverse Hankel

transformation can be fulfilled by a direct numerical integration without paying special attention to the complex singularities.

2.3 Construction of the second kind of Fredholm integral equation for the pile subjected to SH waves

We now derive the second kind of Fredholm integral equation for a pile embedded in the half-space porous medium. Suppose the pile is subjected to a harmonic plane SH wave propagating inside the half-space and the normal of the wave front is parallel to yoz plane (Figure 1). The pile and the surrounding porous medium are assumed to be fully bonded. In terms of the methodology of Muki (1970) and Pak and Jennings (1987), the present problem (Figure 1) is decomposed into two sub-problems: an extended saturated half-space porous medium and a fictitious beam (Figure 3). As mentioned previously, the response of the half-space porous medium is governed by Biot's theory, while the pile is described by a 1D beam vibration theory. Since Halpern and Christiano (Halpem and Christiano, 1986) found that a negligible difference exists between the vertical compliances and load transfer mechanism of impermeable and fully permeable rigid plates on a poroelastic half-space in the low-frequency range, it is reasonable to assume that the influence of the exact hydraulic boundary condition at the contact pile-soil surface is not significant on the response. Consequently, the hydraulic boundary condition on the pile-soil interface is neglected in this study.

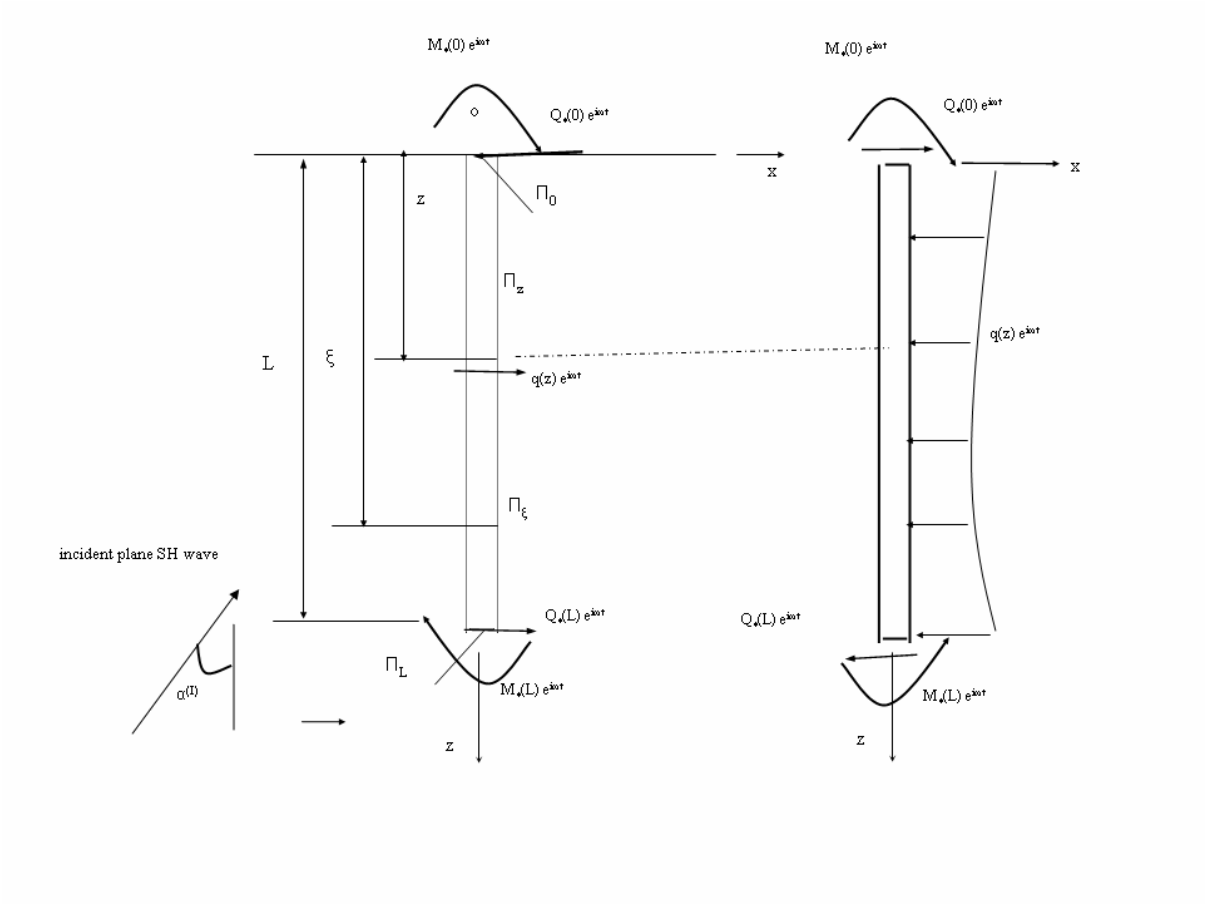

Figure 3 Calculation model for a single pile embedded in a poroelastic half-space and subjected to a plane SH wave.

According to Muki (1970) and Pak and Jennings (1987), the Young's modulus and the density of the fictitious are

$$E_{p*} = E_p - E_s\,,\ \rho_{p*} = \rho_p - \rho_b \tag{29}$$

where E_p and E_s are Young's modulus for the pile and the half-space porous medium, ρ_p, ρ_b are the densities for the pile and the half-space, while E_{p*} and ρ_{p*} are the Young's modulus and the density for the fictitious pile.

Let the shear force and the moment for the fictitious pile to be $Q_*(z)e^{i\omega t}$ and $M_*(z)e^{i\omega t}$, respectively. Moreover, suppose the horizontal load along the fictitious pile is $q(z)e^{i\omega t}$. The top and bottom of the fictitious pile are subjected to the following shear forces and moments: $Q_*(0)e^{i\varpi t}$, $M_*(0)e^{i\varpi t}$ and $Q_*(L)e^{i\varpi t}$, $M_*(L)e^{i\varpi t}$, respectively (Figure 3). According to Newton's third law, the half-space porous medium are subjected to the following forces: over

circular domain Π_z, $q(z)e^{i\omega t}$ is uniformly distributed (Figure 3); at the circular domain Π_0, the half space is subjected to $Q_*(0)e^{i\omega t}, M_*(0)e^{i\omega t}$ (Figure 3); at Π_L, the half space is subjected to shear force $Q_*(L)e^{i\omega t}$ and moment $M_*(L)e^{i\omega t}$.

Following Pak's analysis (Pak and Jennings, 1987),, for piles with larger length and radius ratio, the following equations hold

$$M_*(0) = 0 \ , \ M_*(L) = 0 \, . \tag{30}$$

The above equations simplify numerical calculation significantly. For the fictitious pile, the displacement, the distributed horizontal force, $q(z)e^{i\omega t}$, shear force and moment fulfill the following constraints

$$q(z) = -\frac{dQ_*(z)}{dz} + \rho_{p*} A\omega^2 u_p(z) \, , \tag{31a}$$

$$\frac{dM_*(z)}{dz} = Q_*(z) \, , \tag{31b}$$

where A is the area of the pile cross section, ω is the frequency of the incident wave. Note that for simplicity, the common time factor $e^{i\omega t}$ is omitted in the above equation and it will be omitted in the remainder of the paper.

In the beam theory, the moment, the horizontal displacement and the rotary angle of the pile axis with respect to z axis are as follows

$$M_*(z) = \int_0^z Q_*(\xi) d\xi \, , \tag{32a}$$

$$\theta_p(z) = \frac{1}{E_{p*} I} \int_0^z (z - \xi) Q_*(\xi) d\xi + \theta_0 \, , \tag{32b}$$

$$u_p(z) = \frac{1}{2E_{p*} I} \int_0^z (z - \xi)^2 Q_*(\xi) d\xi + \theta_0 z + u_p(0) \, , \tag{32c}$$

where θ_0 and $u_p(0)$ are the rotary angle and the horizontal displacement at the pile top, I is the second moment of the pile cross section. Note that when deriving (32), the inertia term in (31a) is assumed to be negligible. This assumption is reasonable, because the difference between the density of the pile and the half space porous medium is small and also seismic wave is one kind of low frequency wave.

As mentioned above, it is assumed that the pile and half space are fully bonded. The equality of the rotary angle of the pile axis and the counterpart quantity of the extended half space at z-axis is used as the compatibility condition between the pile and the porous medium (Figure 3):

$$\theta_p(z) = \theta_s(z) \quad ,0 < z < L\,, \tag{33}$$

where $\theta_p(z)$ and $\theta_s(z)$ represent the rotary angle of the fictitious pile axis and the rotary angle of the half-space along z axis, respectively.

The rotary angle of the half-space porous medium along the z axis is composed of two parts: the first part is due to the free wave field, while the second part is due to the force exerted to the half space by the fictitious pile (Figure 3). As a result, if taking into account (30), the rotary angle of the half-space porous medium along the z axis has the following expression

$$\theta_s(z) = \theta_f(z) - Q_*(0)\phi_q(0,z) + Q_*(L)\phi_q(L,z) + \int_0^L q(\xi)\phi_q(\xi,z)d\xi\,, \tag{34}$$

where $\theta_f(z)$ is the free field rotary angle at the z axis, $\phi_q(\xi,z)$ represents the rotary angle at point z due to the unit patch load at Π_ξ. For an incident wave with incident angle $\alpha^{(I)}$ and displacement amplitude $A^{(I)}$ (Figure 1), the free field displacement has the form

$$u_x^{(f)}(y,z)e^{i\omega t} = A^{(I)}[e^{-ik_t(y\sin\alpha^{(I)} - z\cos\alpha^{(I)})} + e^{-ik_t(y\sin\alpha^{(I)} + z\cos\alpha^{(I)})}]e^{i\omega t}\,, \tag{35}$$

where shear wave number k_t is given by (15). Obviously, the above free field fulfills the free surface condition.

Differentiating (35) with respect to z, the free field rotary angle of the porous medium along z axis is obtained

$$\theta_f(z) = \frac{\partial u_x^{(f)}(0,z)}{\partial z} = 2k_t\cos\alpha^{(I)}A^{(I)}\sin(k_t z\sin\alpha^{(I)})\,. \tag{36}$$

Using (31) and integrating (34) by part, the following relation is obtained

$$\theta_S(z) = \theta_f(z) + Q_*(z)[\phi_q(z^+,z) - \phi_q(z^-,z)]$$

$$+\int_0^L Q_*(\xi)\frac{\partial \phi_q(\xi,z)}{\partial \xi}d\xi+\rho_{p*}A\omega^2\int_0^L u_p(\xi)\phi_q(\xi,z)d\xi\,, \tag{37}$$

where $\phi_q(z^-,z),\phi_q(z^+,z)$ denote the rotary angle of the porous medium at z when the patch load Π_ξ approaches Π_z from above and below, respectively. It is worth noting that $\phi_q(z^-,z),\phi_q(z^+,z)$ depend on coordinate z. However, the difference $\phi_q(z^-,z)-\phi_q(z^+,z)$ is independent of coordinate z. As mentioned previously, Π_{z^+}, Π_{z^-} are subjected to uniform patch load with unit resultant, consequently, the following relation holds

$$\sigma_{zx}(z^+,z)-\sigma_{zx}(z^-,z)=\frac{1}{A}, \tag{38}$$

According to the constitutive relation of the porous medium, one has

$$\gamma_{zx}(z^+,z)-\gamma_{zx}(z^-,z)=\frac{1}{\mu A}. \tag{39}$$

As vertical displacement u_z does not experience any variation when the uniform patch load moves from z^- to z^+, consequently, the following relation holds

$$\frac{\partial u_x}{\partial z}(z^+,z)-\frac{\partial u_x}{\partial z}(z^-,z)=\frac{1}{\mu A}, \tag{40}$$

where $\frac{\partial u_x}{\partial z}$ is equal to the rotary angle of the half space porous medium at the z axis.

Using equations (32), (33) and (37), the following second kind of Fredholm integral equation is obtained

$$Q_*(z)[\phi_q(z^+,z)-\phi_q(z^-,z)]+\int_0^L Q_*(\xi)\frac{\partial \phi_q(\xi,z)}{\partial \xi}d\xi-\frac{1}{E_{p*}I}\int_0^z (z-\xi)Q_*(\xi)d\xi$$

$$+\rho_{p*}A\omega^2\int_0^L f_1(\xi)\phi_q(\xi,z)d\xi+\theta_0 f_2(z)+u_p(0)f_3(z)=-\theta_f(z), \tag{41}$$

where

$$f_1(\xi)=\frac{1}{2E_{p*}I}\int_0^\xi Q_*(\eta)(\xi-\eta)^2 d\eta\,, \tag{42a}$$

$$f_2(z) = \rho_{p*} A\omega^2 \int_0^{\xi} \xi \phi_q(\xi, z) d\xi - 1, \tag{42b}$$

$$f_3(z) = \rho_{p*} A\omega^2 \int_0^{\xi} \phi_q(\xi, z) d\xi, \tag{42c}$$

where $u_p(0)$ is the horizontal displacement at the pile top, which can be represented by $Q_*(z)$ and θ_0. For the extended half space, the displacement of the center of Π_z along x direction has the following expression

$$u_s(z) = u_s^{(f)}(z) + \int_0^L Q_*(\xi) \frac{\partial k_q(\xi, z)}{\partial \xi} d\xi + \rho_{p*} A\omega^2 \int_0^L u_p(\xi) k_q(\xi, z) d\xi, \tag{43}$$

where $k_q(\xi, z)$ denotes the horizontal displacement at the center of Π_z due to the unit uniform load at Π_ξ. Substituting (32c) into the above equation and assuming $u_s(0) = u_p(0)$, one obtains

$$u_p(0) = \frac{1}{\delta}[u_s^{(f)}(0) + \int_0^L Q_*(\xi) \frac{\partial k_q(\xi, 0)}{\partial \xi} d\xi + \rho_{p*} A\omega^2 \int_0^L f_1(\xi) k_q(\xi, 0) d\xi$$

$$+ \theta_0 \rho_{p*} A\omega^2 \int_0^L \xi k_q(\xi, 0) d\xi], \tag{44}$$

where $\delta = 1 - \rho_{p*} A\omega^2 \int_0^L k_q(\xi, 0) d\xi$.

Using (30), (32), we have the following relation

$$\int_0^L Q_*(\xi) d\xi = 0. \tag{45}$$

Using integral equation (41) and supplementary equations (44), (45), the shear force, the top rotary angle θ_0 and the top displacement $u_p(0)$ of the fictitious pile can be calculated. The shear force, moment of the real pile and the pore pressure along the real pile side can be evaluated simply by using the obtained shear force, the top rotary angle and the top displacement of the fictitious pile. The shear force of the real pile is equal to the

superposition of the shear force of the fictitious pile and the shear force experienced by the circular domain Π_z

$$Q(z) = Q^{(f)}(z) + Q_*(z) - Q_*(0)\, f_q(0,z) + Q_*(L)\, f_q(L,z) + \int_0^L q(\xi)\, f_q(\xi,z) d\xi\,, \qquad (46)$$

where $f_q(\xi,z)$ represents the shear force applied on Π_z due to a uniform patch load at Π_ξ. Inserting (31a) and (32c) into above equation and integrating above equation by part yields the following equation

$$Q(z) = Q^{(f)}(z) + \rho_{p*} A\omega^2 \int_0^L f_1(\xi)\ f_q(\xi,z) d\xi\ + \int_0^L Q_*(\xi) \frac{\partial f_q(\xi,z)}{\partial \xi} d\xi +$$

$$[\rho_{p*} A\omega^2 \int_0^L \xi\ f_q(\xi,z) d\xi\ ]\theta_0 + [\rho_{p*} A\omega^2 \int_0^L\ f_q(\xi,z) d\xi\ ] u_p(0) \qquad (47)$$

Note that when deriving the above equation, the relation $f_q(z^+,z) - f_q(z^-,z) = -1.0$ is used. Likewise, pore pressure at the pile side can be evaluated by the following equation

$$p(z) = \int_0^L Q_*(\xi) \frac{\partial p_q(\xi,z)}{\partial \xi} d\xi + \rho_{p*} A\omega^2 \int_0^L f_1(\xi)\ p_q(\xi,z) d\xi$$

$$+ [\rho_{p*} A\omega^2 \int_0^L \xi\ p_q(\xi,z) d\xi\ ]\theta_0 + [\rho_{p*} A\omega^2 \int_0^L\ p_q(\xi,z) d\xi] u_p(0) \qquad (48)$$

where $p_q(\xi,z)$ is the pore pressure at the circumference of Π_z due to a unit patch load at Π_ξ. Note that as the dilatations of the fluid and the solid vanish when subjected to SH waves, consequently, the free field has no contribution to the pore pressure at the pile side. The moment of the real pile is the superposition of the moment of the fictitious pile and the moment experienced by section Π_z. Alternatively, the moment of the real pile can be evaluated by integrating the shear force of the real pile.

2.4 Numerical Scheme

The integral equation (41) can be discretised by *n* uniformly distributed discrete points. Consequently, there are *n* discrete unknown fictitious shear forces. Besides, the top

displacement $u_p(0)$ and rotary angle θ_0 of the fictitious pile are also unknown. Hence, the total number of unknown parameters is *n*+2. Discretization of the integral equation (41) will generate *n* algebraic equations. The *n* algebraic equations together with supplementary equations (44) and (45) determine the numerical solutions for the *n*+2 unknowns. The methodology for solving integral equation (41) was detailed by Boonsrang and Pisidhi (1981) and Lu (2000). The numerical stability of the approach for solving this kind of integral equation is demonstrated by Boonsrang and Pisidhi (1981) and Lu (2000).

3. Results and Discussions

3.1 Comparison of the results of a porous medium with a single phase elastic medium

In this example, the difference between the porous medium and single phase elastic medium is considered. The displacement, rotary angle and shear force of a pile surrounded by a porous medium and a single phase medium are calculated. The incident angle of the incident plane SH wave is equal to 60^0 (Figure 1), and the incident SH wave is tuned to make free field rotary angle of the medium at the bottom of the pile have unit value. The frequency of the incident SH wave is 100 Hz. The radius *R* of the pile is 0.25 m, while the length and radius ratio of the pile equals to 80. The Young's modulus of the pile equals to $E_p = 1.0\times10^{10}$ Pa. The parameters are taken as follows for the porous medium

$$\mu = 3.0\times10^7 \text{ Pa},\ \lambda = 1.0\times10^7 \text{ Pa},\ \rho_s = 2.5\times10^3 \text{ kg/m}^3,\ \rho_f = 1.0\times10^3 \text{ kg/m}^3,$$

$$K_m = 10.0\times10^9 \text{ Pa},\ K_f = 2.5\times10^9 \text{ Pa},\ \phi = 0.3,\ \eta = 1.0\times10^{-3} \text{ Pa.s},\ k = 1.0\times10^{-12} \text{ m}^2 \qquad (49)$$

where K_m and K_f are the bulk modulus for the material of the solid skeleton and the pore fluid. The parameters α, M involved in the constitutive relation of the porous medium (1) can be evaluated by the Gassmann's equation (Gassmann, 1951) and unjacketed and undrained test of Biot's theory (Biot, 1957). If we assume that the unjacketed modulus of the porous medium is equal to the material bulk modulus of the solid skeleton, then, in terms of Biot's theory (Biot, 1962), α, M have the following expressions

$$\alpha = \frac{K_m - K}{K_m},\ M = \frac{(K_G - K)K_m^2}{K^2 - 2KK_m + K_m^2}, \qquad (50)$$

where $K = \lambda + 2\mu/3$ and K_G is undrained bulk modulus of the porous medium which can be determined by Gassmann's equation (Gassmann, 1951) by using K, K_m, K_f as well as the porosity of the porous medium. Consequently, according to Gassmann's equation (Gassmann, 1951), for the above porous medium, α, M assume 0.997 and 5.2715×10^9 Pa, respectively. On the other hand, if let parameters M, ρ_f, b, α, ϕ tend to zero, then, the porous medium here is reduced to a single phase elastic medium. In calculation, the pile is discretized into 50 segments. It is noted that when calculating fundamental solutions for the single phase medium, to avoid real Rayleigh equation root, 2 percent of the imaginary part is added to the modulus λ, μ (Luco and Apsel, 1983). Physically, it will bring about non-causal numerical results. However, it is negligible due to the small imaginary part of the modulus. The displacement, rotary angle and shear force of the pile for the two cases are presented in Figures 4. It follows from Figure 4 that at the upper part of the pile, the displacement and the rotary angle of the porous medium case are larger than those of the elastic single phase case, whereas at the bottom part of the pile, the displacement and the rotary angle of the porous medium case are smaller than those of the elastic single phase case. Figure 4 (c) shows the maximum of the shear force of the single phase case is larger than the porous medium case.

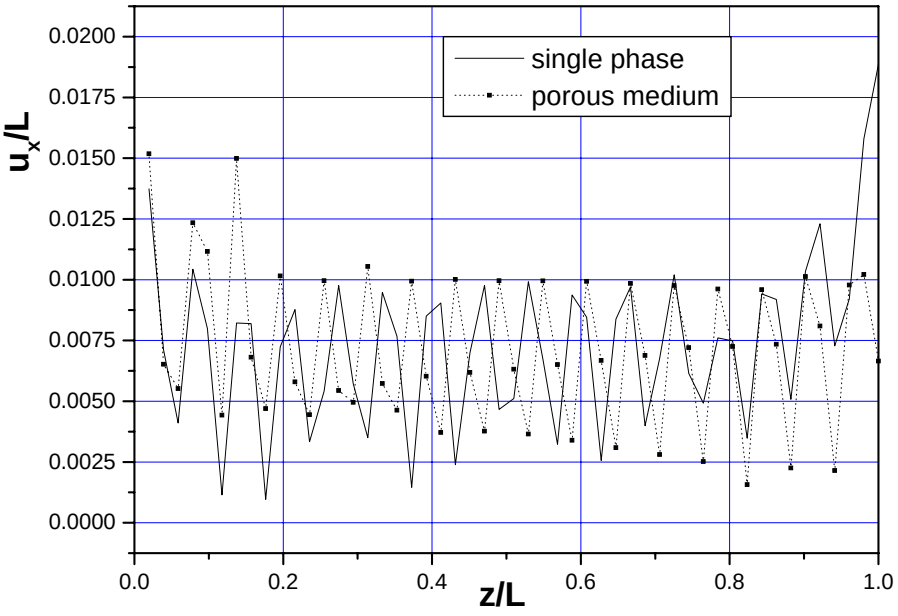
single phase
porous medium
u_x/L
z/L
0.0200
0.0175
0.0150
0.0125
0.0100
0.0075
0.0050
0.0025
0.0000
0.0
0.2
0.4
0.6
0.8
1.0

(a)

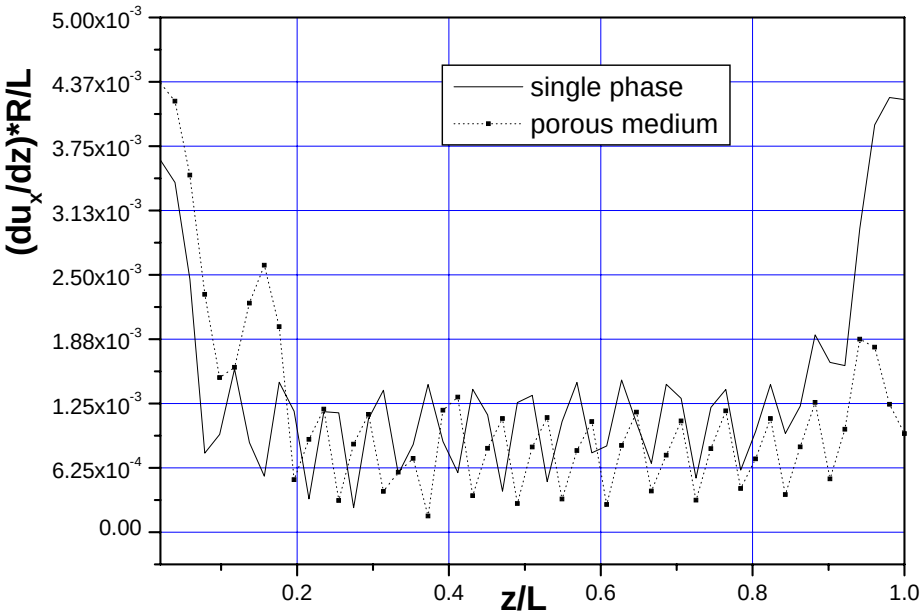
single phase
porous medium
$(du_x/dz)*R/L$
z/L
$5.00x10^{-3}$
$4.37x10^{-3}$
$3.75x10^{-3}$
$3.13x10^{-3}$
$2.50x10^{-3}$
$1.88x10^{-3}$
$1.25x10^{-3}$
$6.25x10^{-4}$
0.00
0.2
0.4
0.6
0.8
1.0

(b)

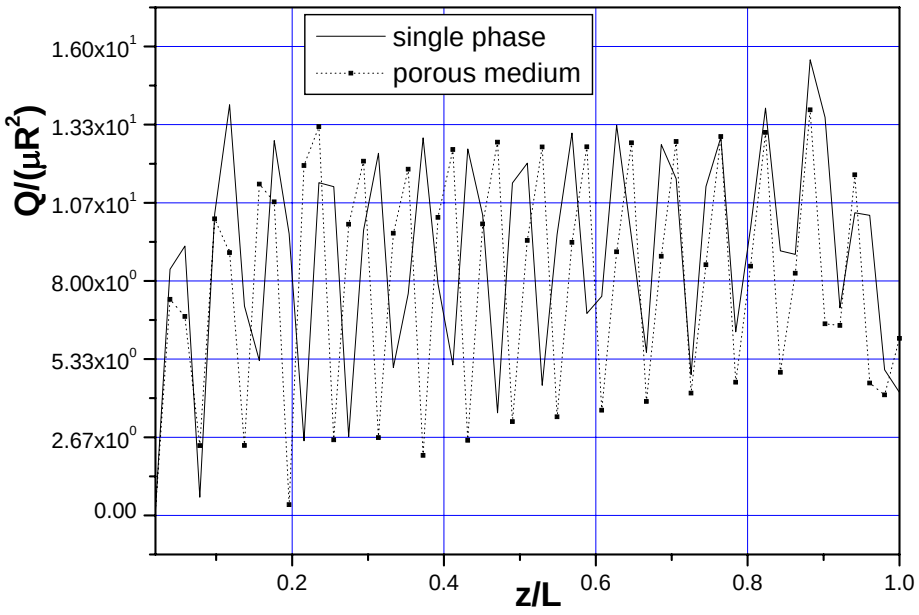

(c)

Figure 4 Comparison of the response of a pile embedded in a porous medium and a single phase medium: (a) horizontal displacement of the pile axis u_x / L for porous medium and single phase medium; (b) the rotary angle of the pile axis $(du_x / dz)R / L$ for porous medium and single phase medium; (c) the shear force of the pile $Q/(\mu R^2)$ for porous medium and single phase medium.

3.2 The influence of the permeability

In this example, the influence of permeability of the porous medium on the dynamic response of the pile will be examined. The displacement, rotary angle and shear force of the pile as well as the pore pressure at the side of the pile for permeability $k = 1.0 \times 10^{-10}\,\mathrm{m}^2$, $k = 1.0 \times 10^{-11}\,\mathrm{m}^2$, $k = 1.0 \times 10^{-12}\,\mathrm{m}^2$ are calculated. The incident angle of the incident plane SH wave is equal to 60^0 (Figure 1), and the incident SH wave is tuned to make free field rotary angle of the porous medium at the bottom of the pile have unit value. The frequency of the incident SH wave takes 10 Hz, 100 Hz and 1000 Hz, respectively. The radius *R* of the pile is 0.25 m, while the length and radius ratio of the pile equals to 80. The Young's modulus of the pile is equal to $E_p = 1.0 \times 10^9$ Pa. For the porous medium surrounding the pile, the parameters are taken as follows

$$\mu = 3.0\times10^{7}\ \text{Pa},\quad \lambda = 1.0\times10^{7}\ \text{Pa},\ \rho_s = 2.5\times10^{3}\ \text{kg/m}^3,\ \rho_f = 1.0\times10^{3}\ \text{kg/m}^3,$$

$$K_m = 5.0\times10^{9}\ \text{Pa},\ K_f = 2.5\times10^{9}\ \text{Pa},\ \phi = 0.3,\quad \eta = 1.0\times10^{-3}\ \text{Pa.s}, \tag{51}$$

where K_m and K_f are the bulk modulus for the material of the solid skeleton and the pore fluid. According to Gassmann's equation (Gassmann, 1956) and Biot's theory (Biot, 1956b), the parameters α, M take 0.994 and 3.8640×10^{9} Pa, respectively. In calculation, the pile is discretized into 50 segments. The displacement, rotary angle of the pile axis, shear force of the pile and pore pressure along the pile side are plotted in Figures 5-7.

Figure 5 shows for incident wave with frequency 10 Hz, except the pore pressure, the displacement, the rotary angle and the shear force of the pile do not have large difference for the three cases $k = 1.0\times10^{-10}$ m^2, 1.0×10^{-11} m^2, 1.0×10^{-12} m^2. However, with decreasing permeability, the pore pressure increases dramatically, in particular at the domains near the top and the bottom of the pile. For incident wave with frequency 100 Hz, the amplitudes of displacement, rotary angle, shear force and pore pressure increase with decreasing permeability. Nevertheless, the differences of displacement, rotary angle, shear force between the two cases $k = 1.0\times10^{-11}$ m^2 and $k = 1.0\times10^{-12} m^2$ m^2 are difficult to observed. For 1000 Hz incident wave, the rotary angle of the pile increases with decreasing permeability. The amplitudes of displacement, shear force and pore pressure of the case $k = 1.0\times10^{-12}$ m^2 are the largest among the three cases, while those for $k = 1.0\times10^{-10}$ m^2 is the second largest and the case $k = 1.0\times10^{-11}$ m^2 are the smallest. Moreover, with increasing frequency, the displacement and the rotary angle of the pile decrease. Besides, for the incident wave with frequency f=100 Hz, the shear force and pore pressure are the largest among the three cases.

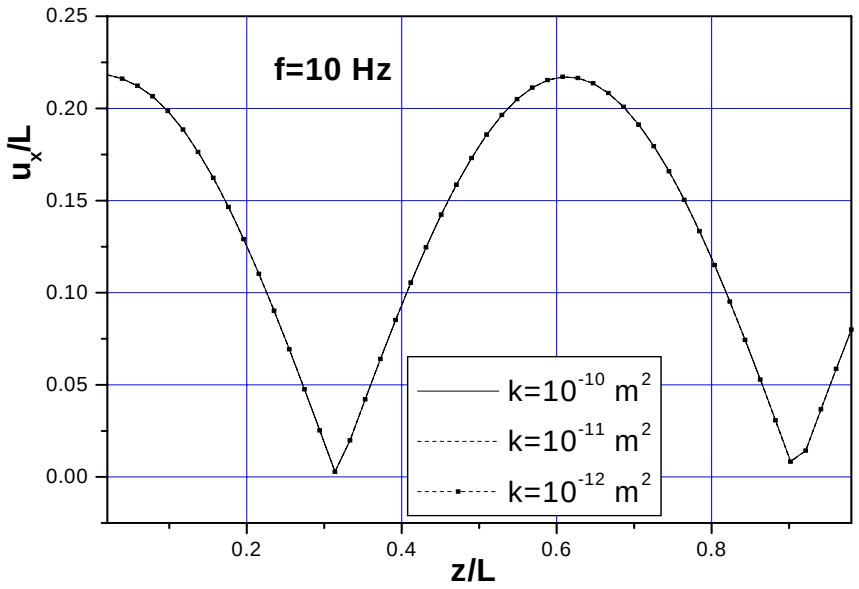
f=10 Hz
u_x/L
z/L
0.25
0.20
0.15
0.10
0.05
0.00
0.2
0.4
0.6
0.8
k=10^{-10} m^2
k=10^{-11} m^2
k=10^{-12} m^2

(a)

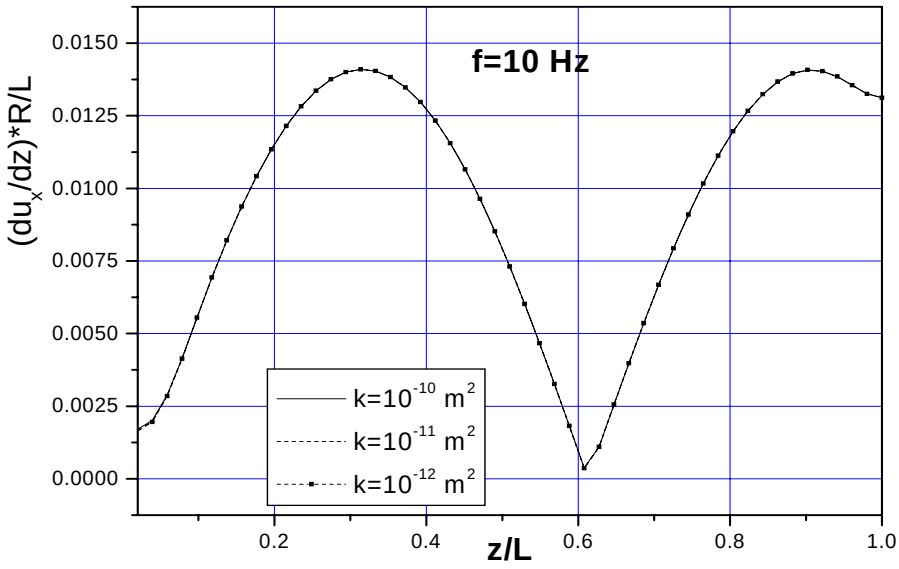
f=10 Hz
$(du_x/dz)*R/L$
z/L
0.0150
0.0125
0.0100
0.0075
0.0050
0.0025
0.0000
0.2
0.4
0.6
0.8
1.0
k=10^{-10} m^2
k=10^{-11} m^2
k=10^{-12} m^2

(b)

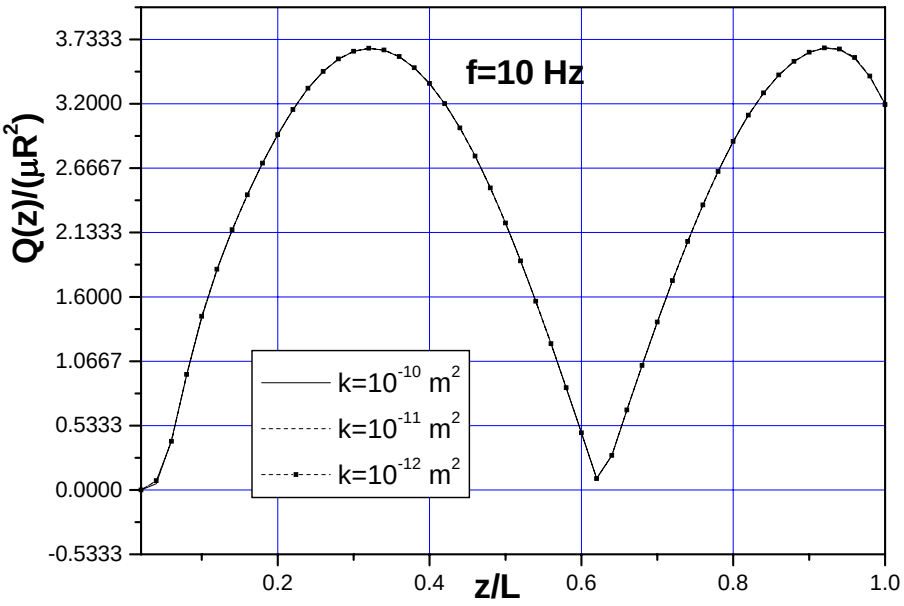

(c)

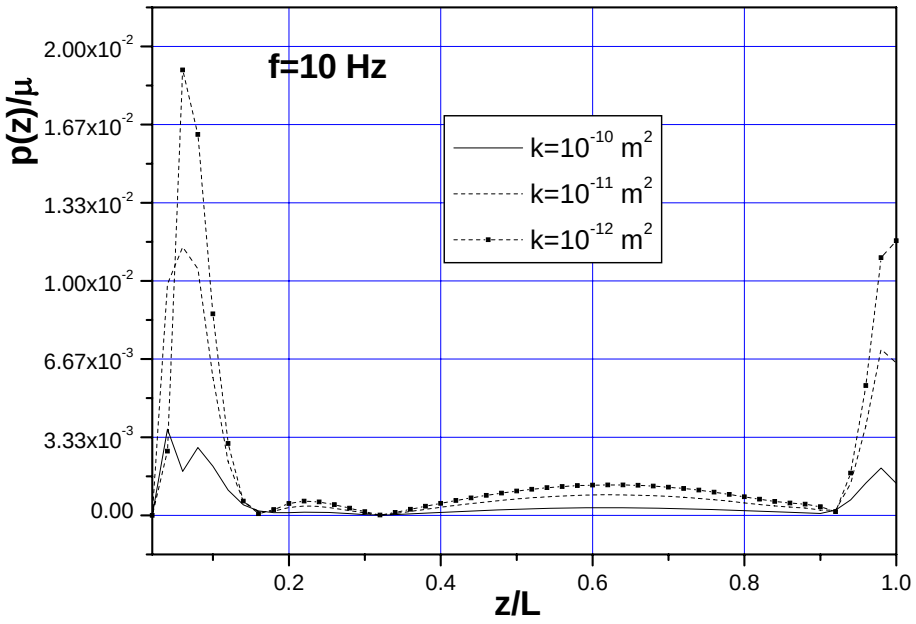

(d)

Figure 5 The influence of the permeability ($k = 1.0\times10^{-10}m^2, 1.0\times10^{-11}m^2, 1.0\times10^{-12}m^2$) on the dynamic response of a pile subjected to a plane SH wave with frequency equal to 10 Hz: (a) horizontal displacement of the pile axis u_x / L; (b) the rotary angle of the pile axis $(du_x / dz)R / L$; (c) the shear force of the pile $Q/(\mu R^2)$; (d) the pore pressure along the side of the pile p / μ.

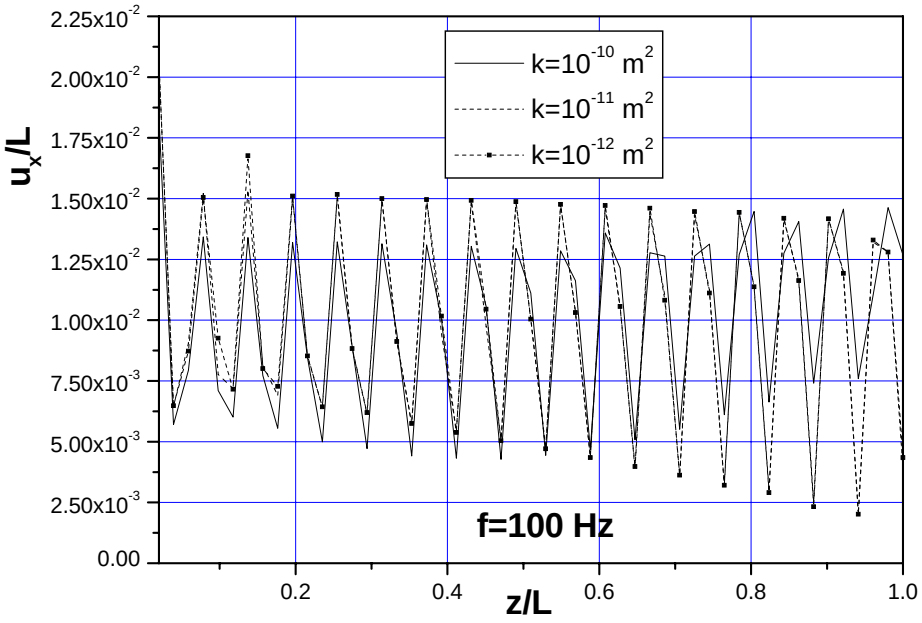
2.25x10-2
2.00x10-2
1.75x10-2
1.50x10-2
1.25x10-2
1.00x10-2
7.50x10-3
5.00x10-3
2.50x10-3
0.00
ux/L
k=10-10 m2
k=10-11 m2
k=10-12 m2
f=100 Hz
0.2
0.4
0.6
0.8
1.0
z/L

(a)

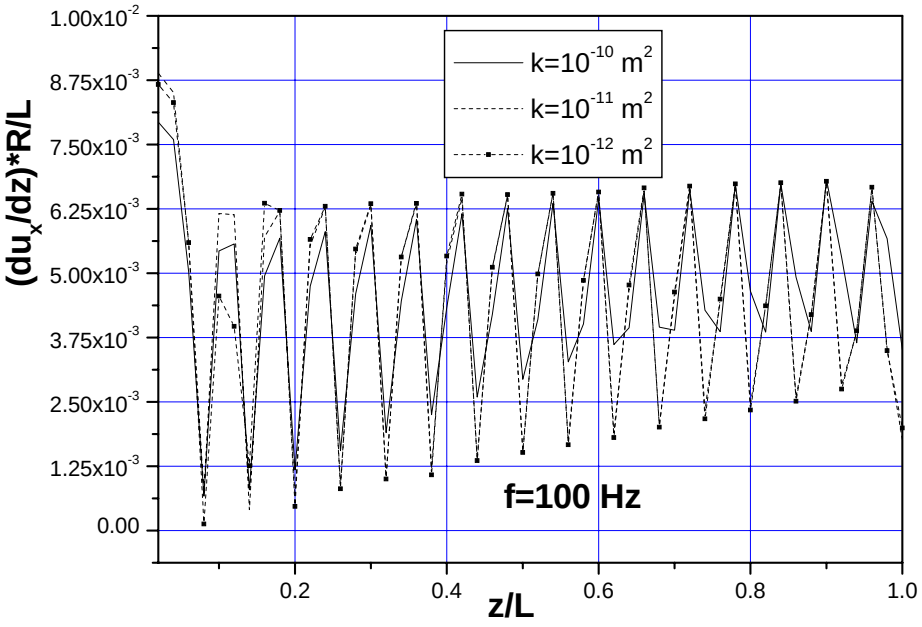
1.00x10-2
8.75x10-3
7.50x10-3
6.25x10-3
5.00x10-3
3.75x10-3
2.50x10-3
1.25x10-3
0.00
(dux/dz)*R/L
k=10-10 m2
k=10-11 m2
k=10-12 m2
f=100 Hz
0.2
0.4
0.6
0.8
1.0
z/L

(b)

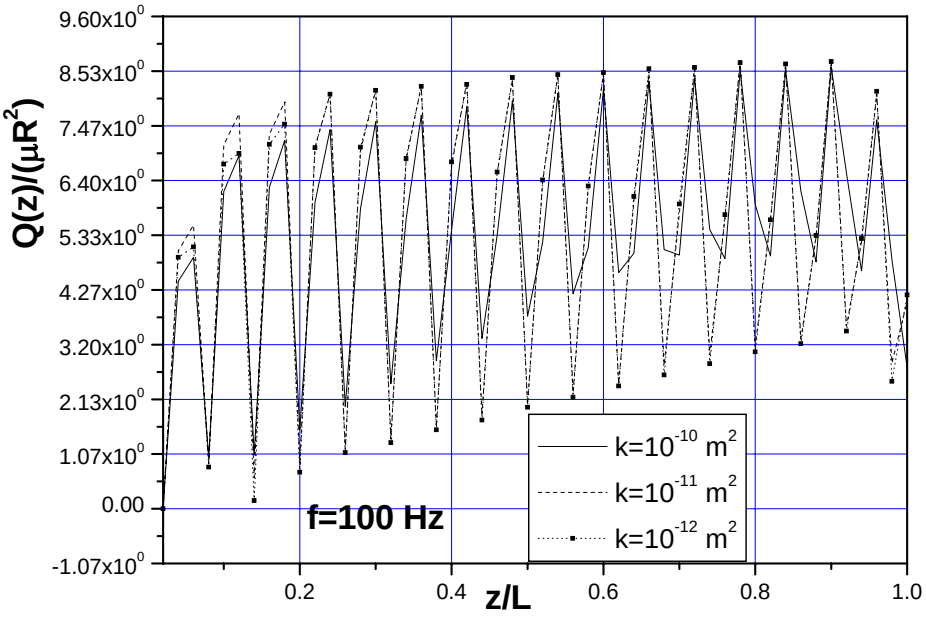

(c)

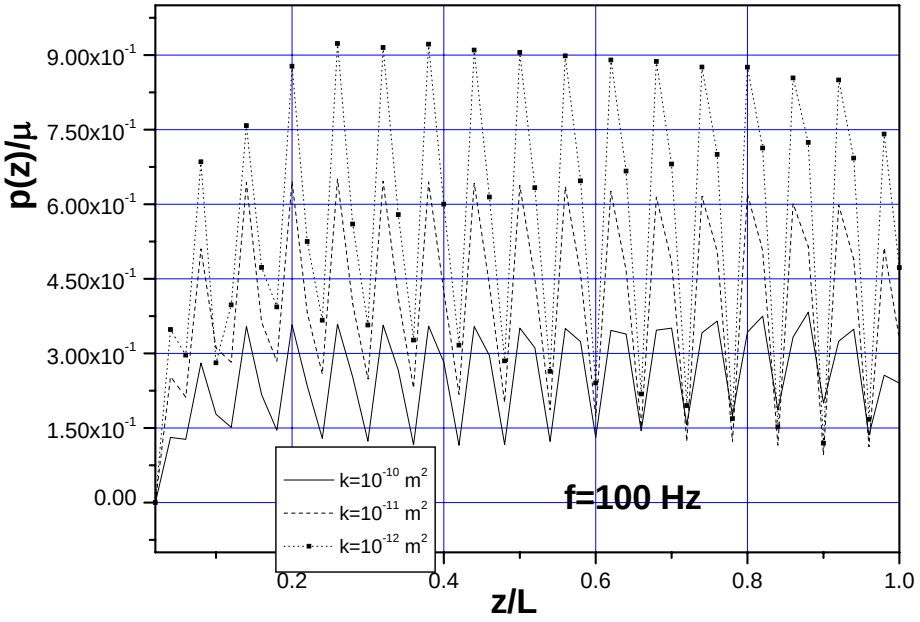

(d)

Figure 6 The influence of the permeability ($k = 1.0\times10^{-10} m^2, 1.0\times10^{-11} m^2, 1.0\times10^{-12} m^2$) on the dynamic response of a pile subjected to a plane SH wave with frequency equal to 100 Hz: (a) horizontal displacement of the pile axis u_x / L; (b) the rotary angle of the pile axis $(du_x / dz)R / L$; (c) the shear force of the pile $Q/(\mu R^2)$; (d) the pore pressure along the side of the pile p/μ.

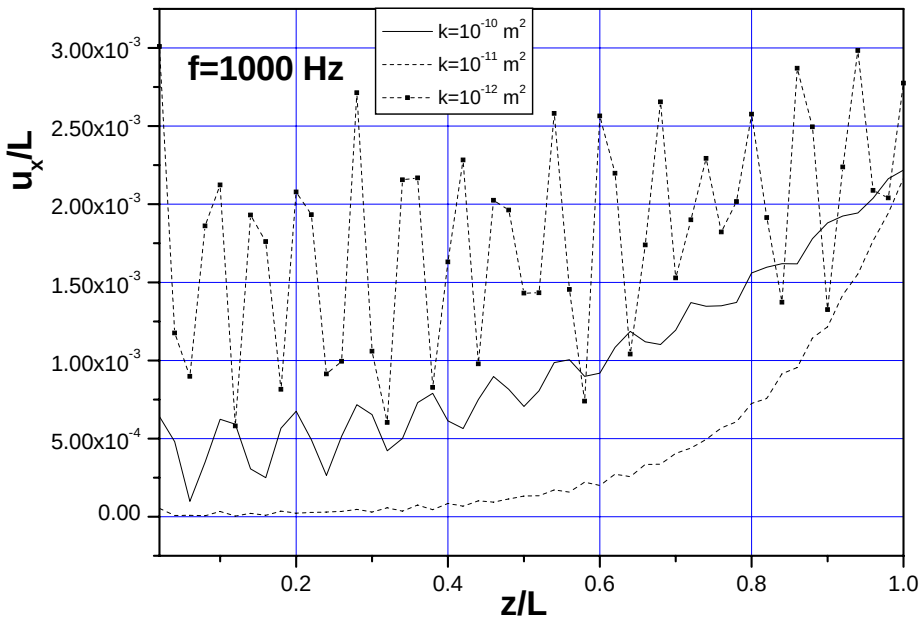
f=1000 Hz
k=10^-10 m^2
k=10^-11 m^2
k=10^-12 m^2
u_x/L
3.00x10^-3
2.50x10^-3
2.00x10^-3
1.50x10^-3
1.00x10^-3
5.00x10^-4
0.00
0.2
0.4
0.6
0.8
1.0
z/L

(a)

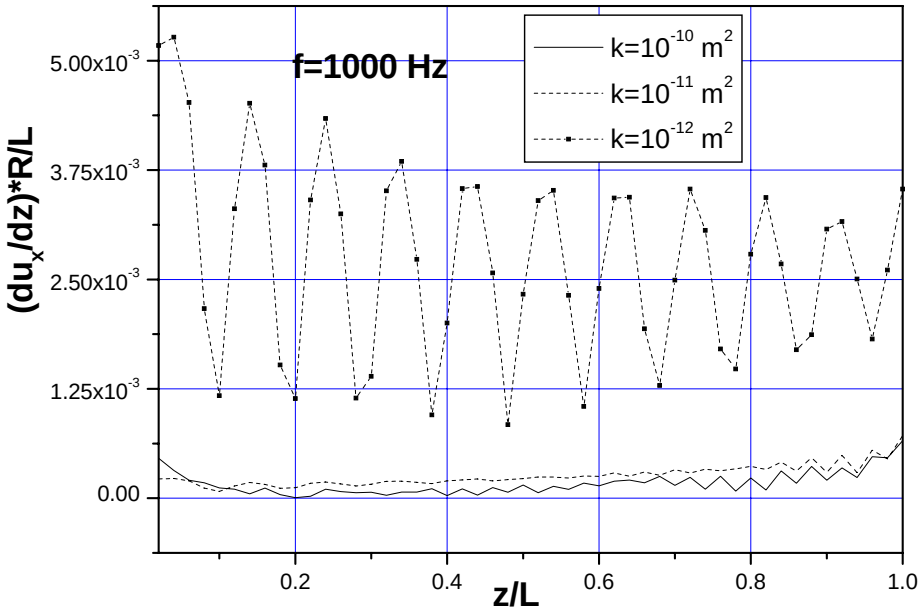
f=1000 Hz
k=10^-10 m^2
k=10^-11 m^2
k=10^-12 m^2
(du_x/dz)*R/L
5.00x10^-3
3.75x10^-3
2.50x10^-3
1.25x10^-3
0.00
0.2
0.4
0.6
0.8
1.0
z/L

(b)

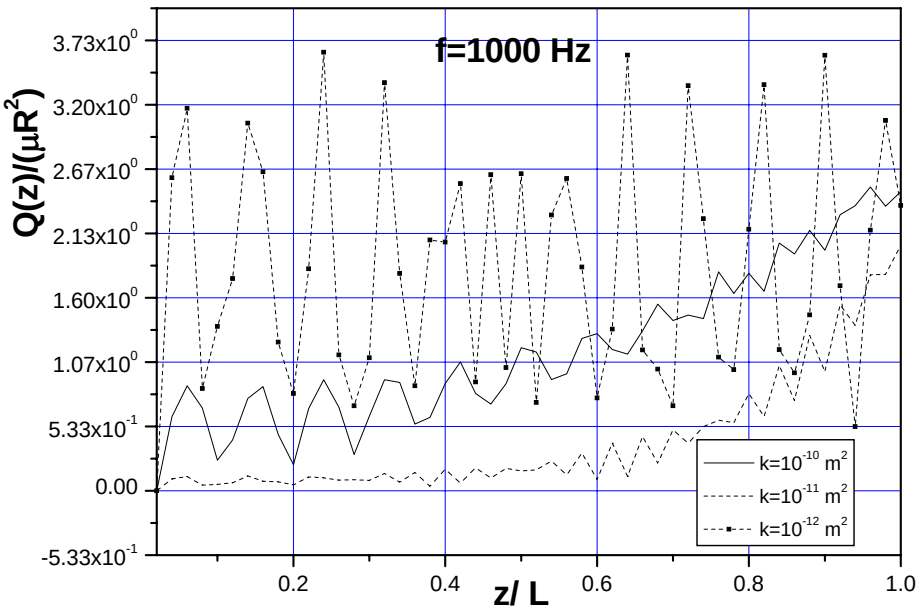

(c)

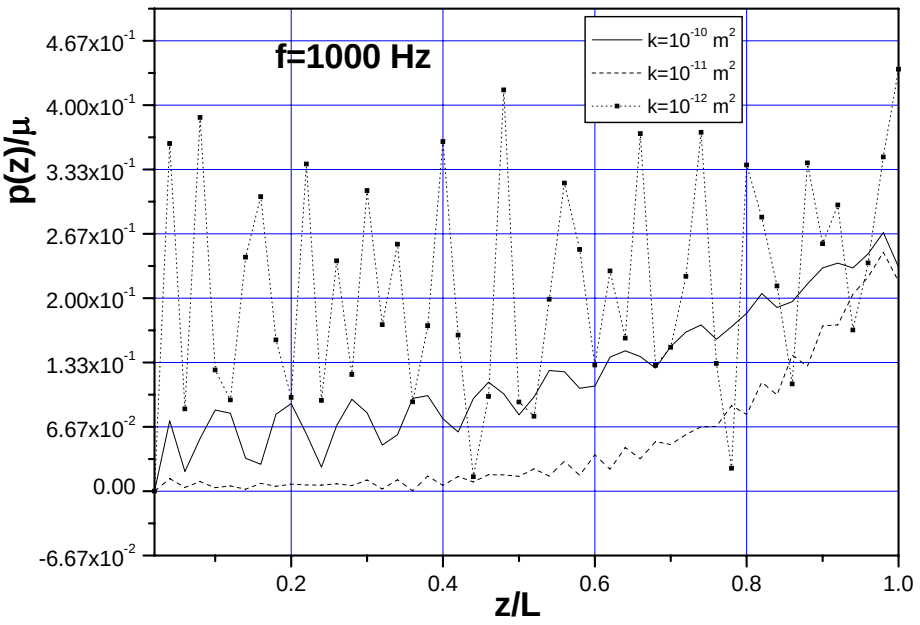

(d)

Figure 7 The influence of the permeability ($k = 1.0\times10^{-10} m^2, 1.0\times10^{-11} m^2, 1.0\times10^{-12} m^2$) on the dynamic response of a pile subjected to a plane SH wave with frequency equal to 1000 Hz: (a) horizontal displacement of the pile axis u_x / L; (b) the rotary angle of the pile axis $(du_x / dz)R / L$; (c) the shear force of the pile $Q/(\mu R^2)$; (d) the pore pressure along the side of the pile p/μ.

3.3 Effect of modulus ratio between the pile and the porous medium

In this example, the effect of the modulus ratio between the pile and the porous medium on the dynamic response of the pile will be investigated. The displacement, rotary angle and shear force along the pile axis as well as the pore pressure at side of the pile for the three cases $E_p / E_s = 10$, $E_p / E_s = 100$, $E_p / E_s = 1000$ are calculated. The incident angle of the incident plane SH wave is equal to 60^0 (Fig.1), and the incident SH wave is tuned to make free field rotary angle of the porous medium at the bottom of the pile have unit value. The frequency of the incident SH wave takes 10 Hz, 100 Hz and 1000 Hz, respectively. The permeability of the porous medium equals to $k = 1.0 \times 10^{-12}$ m^2. All the other parameters for the porous medium and the pile take the same values as Example 3.2. Likewise, in calculation, the pile is discretized into 50 segments. The displacement, rotary angle, the shear force and the pore pressure along the side of the pile are given in Figures 8-10.

For f=10 Hz incident wave, the displacement, rotary angle of the pile axis only have slight difference for the three cases: $E_p / E_s = 10$, $E_p / E_s = 100$, $E_p / E_s = 1000$. However, with increasing E_p / E_s, the shear force and the pore pressure increase significantly. For an incident wave with frequency f=100 Hz, the displacement and rotary angle along the pile axis decrease with increasing E_p / E_s. Conversely, the shear force and the pore pressure increase with increasing E_p / E_s. For SH wave with a frequency f=1000 Hz, the difference of the horizontal displacement between the three cases is minor, whereas the rotary angle decreases greatly with increasing E_p / E_s. With increasing E_p / E_s, the shear force and the pore pressure along the pile side decrease slightly. For SH incident wave with different frequency, again we see the same tendency as in section 3.2: with increasing frequency, the displacement and the rotary angle of the pile decrease; when the incident frequency f=100 Hz, the shear force and pore pressure are the largest among the three cases.

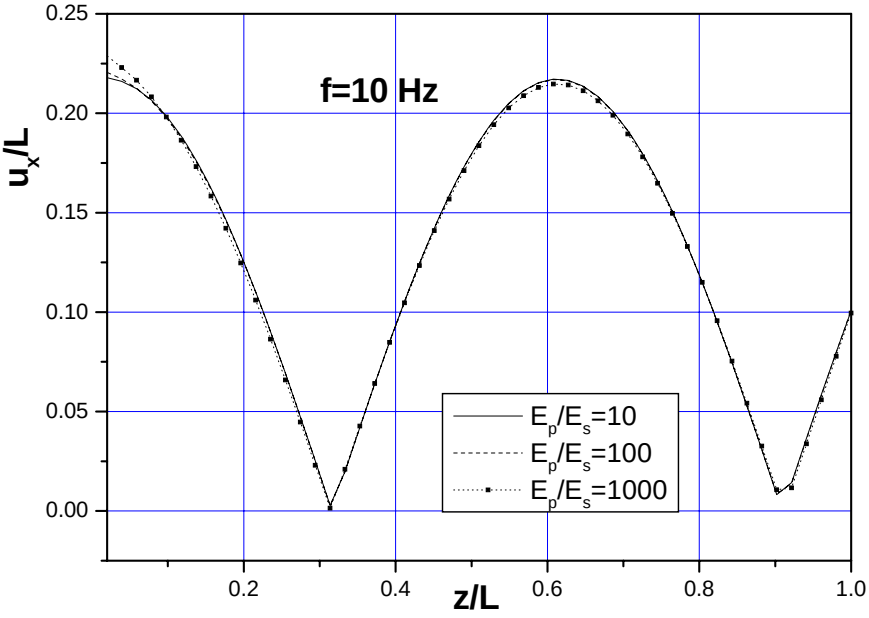
f=10 Hz
u_x/L
z/L
E_p/E_s=10
E_p/E_s=100
E_p/E_s=1000

(a)

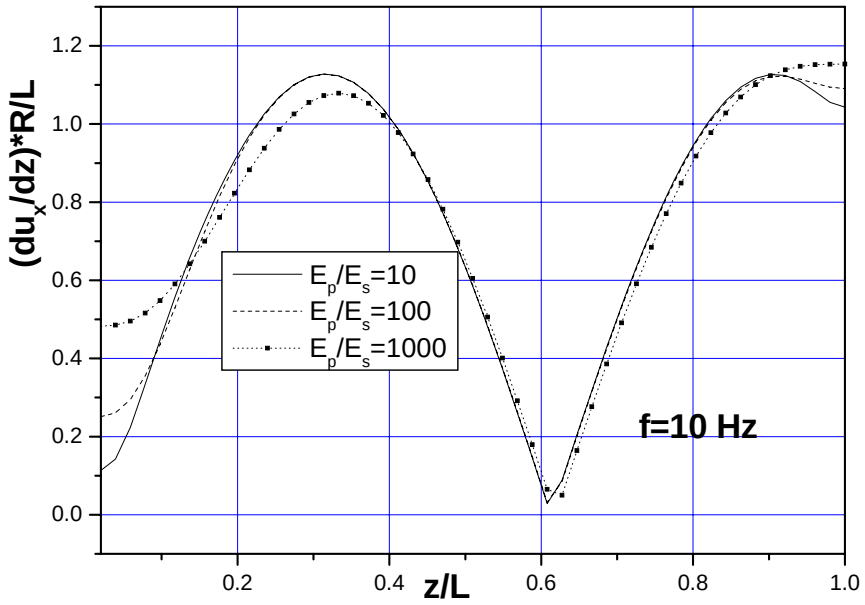
$(du_x/dz)*R/L$
z/L
E_p/E_s=10
E_p/E_s=100
E_p/E_s=1000
f=10 Hz

(b)

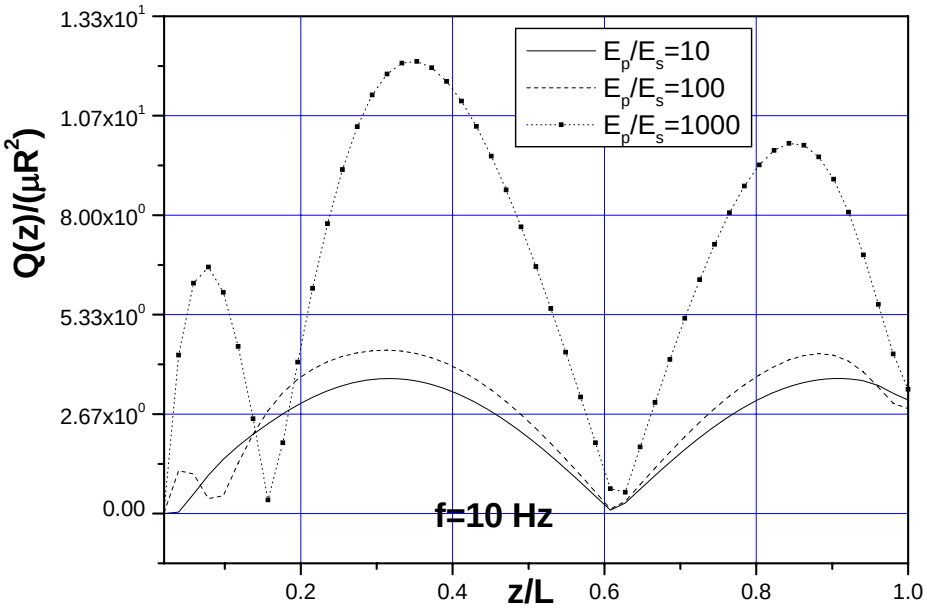

(c)

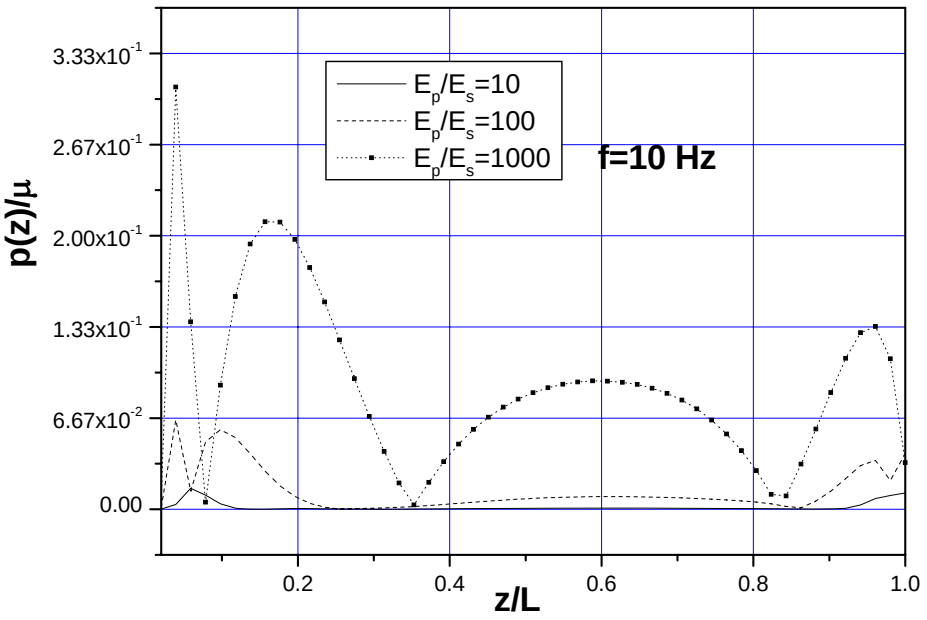

(d)

Figure 8 The influence of the modulus ratio between the pile and the porous medium ($E_p / E_s = 10,100,1000$) on the dynamic response of a pile subjected to a plane SH wave with frequency equal to 10 Hz: (a) horizontal displacement of the pile axis u_x / L; (b) the rotary angle of the pile axis $(du_x / dz)R / L$; (c) the shear force of the pile $Q/(\mu R^2)$; (d) the pore pressure along the side of the pile p / μ.

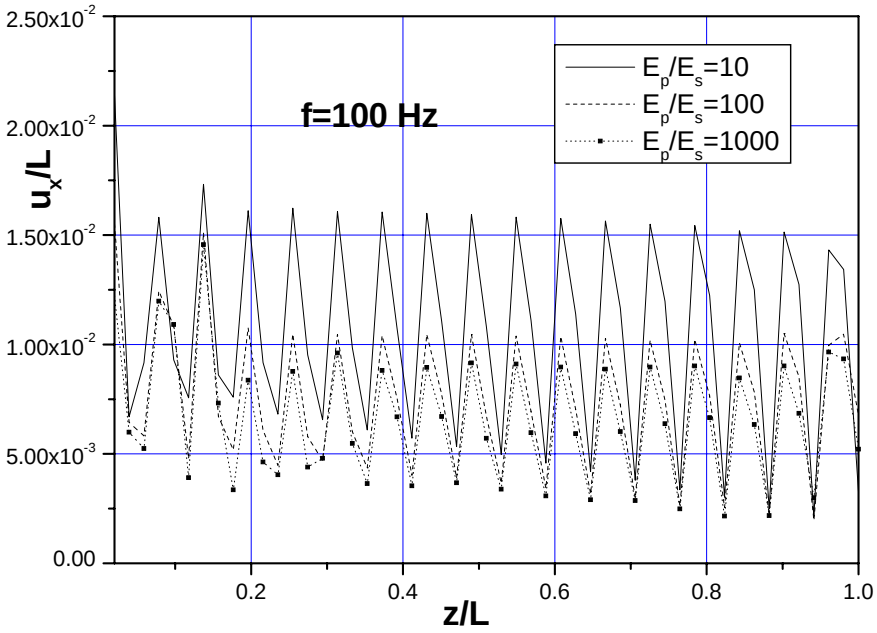
f=100 Hz
E_p/E_s=10
E_p/E_s=100
E_p/E_s=1000
u_x/L
z/L
2.50x10^-2
2.00x10^-2
1.50x10^-2
1.00x10^-2
5.00x10^-3
0.00
0.2
0.4
0.6
0.8
1.0

(a)

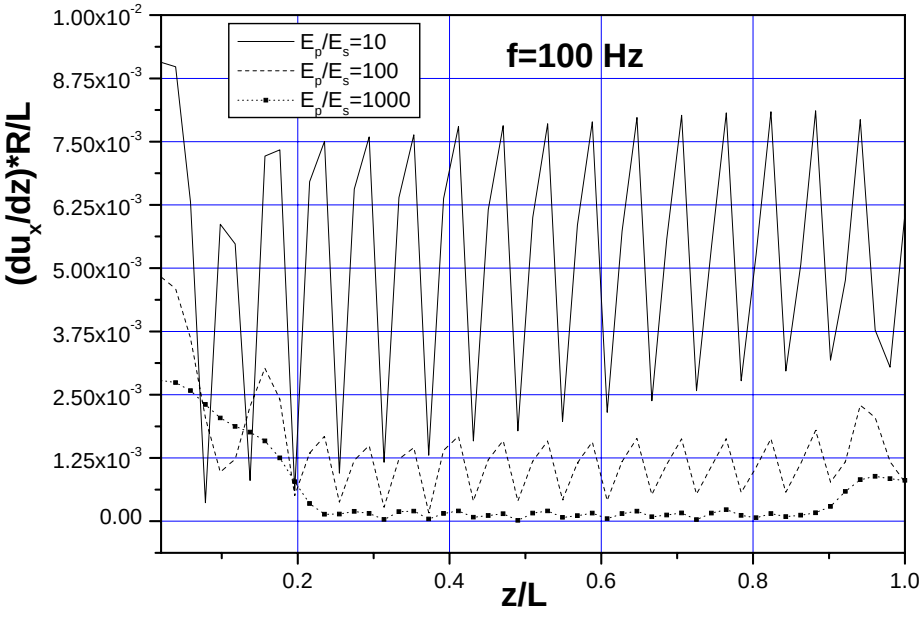
f=100 Hz
E_p/E_s=10
E_p/E_s=100
E_p/E_s=1000
(du_x/dz)*R/L
z/L
1.00x10^-2
8.75x10^-3
7.50x10^-3
6.25x10^-3
5.00x10^-3
3.75x10^-3
2.50x10^-3
1.25x10^-3
0.00
0.2
0.4
0.6
0.8
1.0

(b)

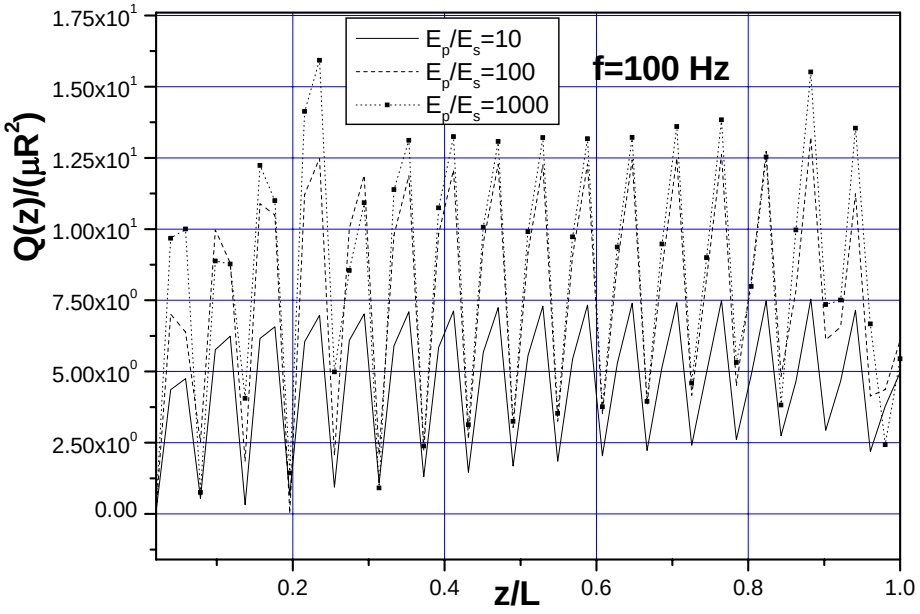

(c)

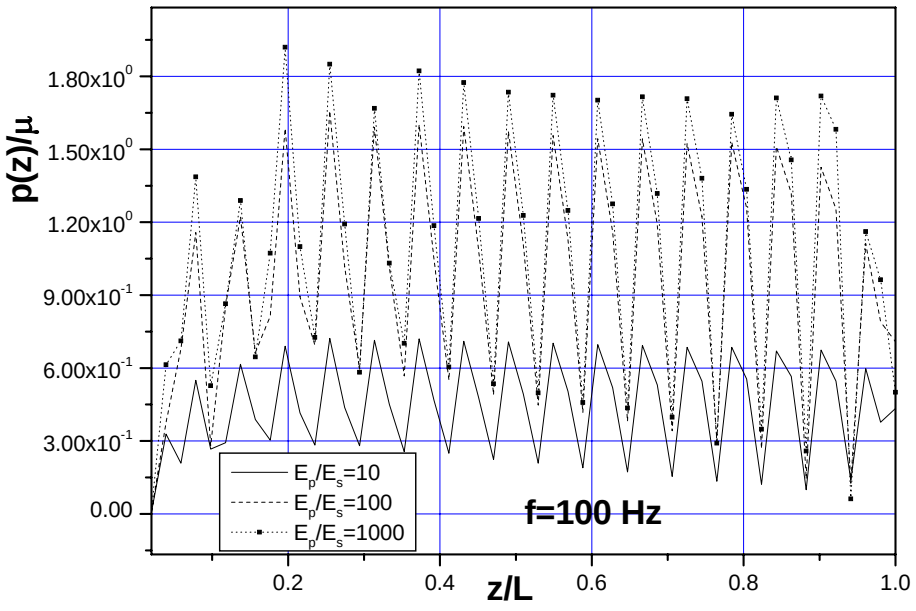

(d)

Figure 9 The influence of the modulus ratio between the pile and the porous medium ($E_p / E_s = 10,100,1000$) on the dynamic response of a pile subjected to a plane SH wave with frequency equal to 100 Hz: (a) horizontal displacement of the pile axis u_x / L; (b) the rotary angle of the pile axis $(du_x / dz)R / L$; (c) the shear force of the pile $Q/(\mu R^2)$; (d) the pore pressure along the side of the pile p / μ.

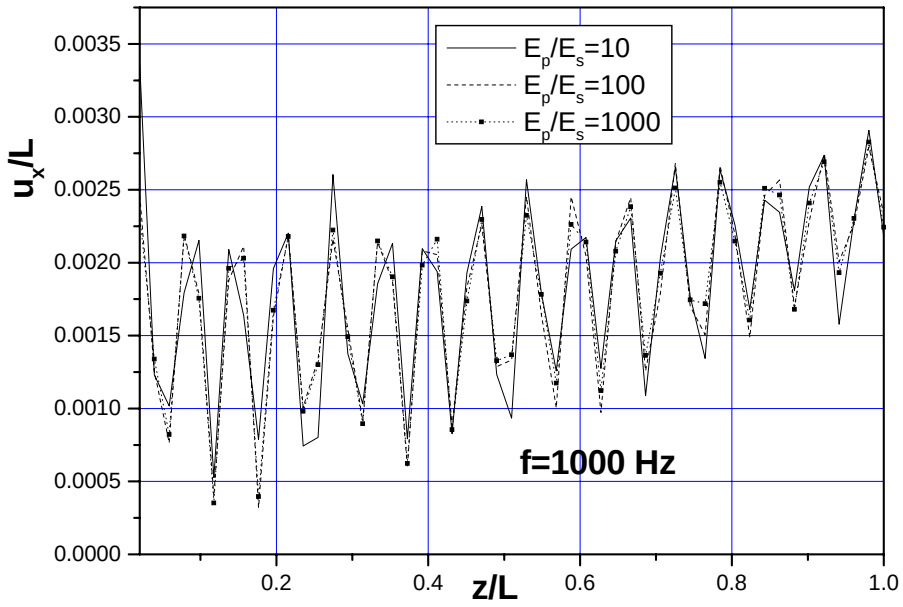
E_p/E_s=10
E_p/E_s=100
E_p/E_s=1000
f=1000 Hz
u_x/L
z/L
0.0035
0.0030
0.0025
0.0020
0.0015
0.0010
0.0005
0.0000
0.2
0.4
0.6
0.8
1.0

(a)

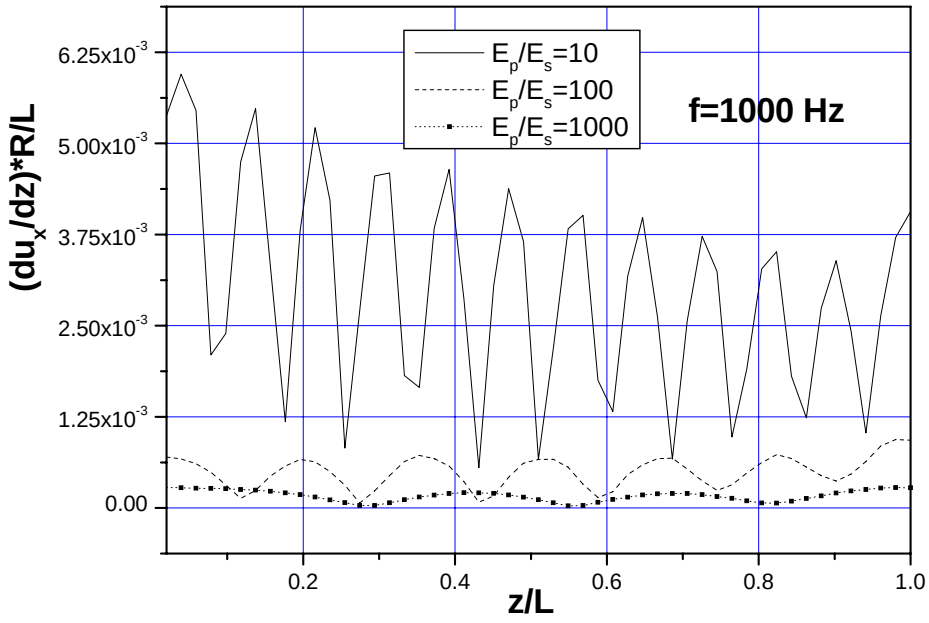
E_p/E_s=10
E_p/E_s=100
E_p/E_s=1000
f=1000 Hz
$(du_x/dz)*R/L$
z/L
$6.25x10^{-3}$
$5.00x10^{-3}$
$3.75x10^{-3}$
$2.50x10^{-3}$
$1.25x10^{-3}$
0.00
0.2
0.4
0.6
0.8
1.0

(b)

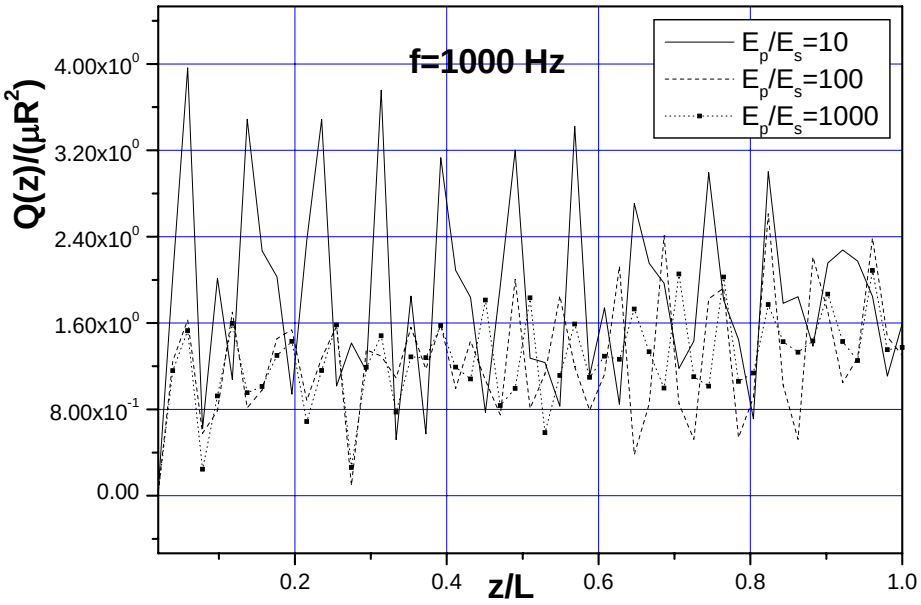

(c)

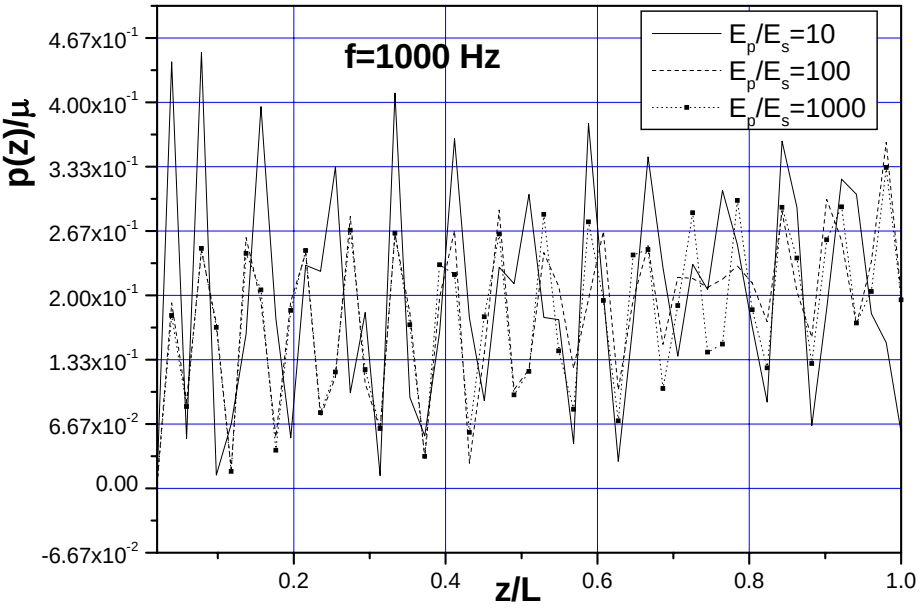

(d)

Figure 10 The influence of the modulus ratio between the pile and the porous medium ($E_p / E_s = 10,100,1000$) on the dynamic response of a pile subjected to a plane SH wave with frequency equal to 1000 Hz: (a) horizontal displacement of the pile axis u_x / L; (b) the rotary angle of the pile axis $(du_x / dz)R / L$; (c) the shear force of the pile $Q/(\mu R^2)$; (d) the pore pressure along the side of the pile p/μ.

4. Conclusions

In this study, employing Biot's theory and integral equation method, the frequency domain dynamic response of a pile to plane SH waves is investigated. Central to our investigation is the establishment of the fundamental solutions and construction of the second kind Fredholm integral equation for the pile. The fundamental solutions involved in the integral equation are established using the Fourier and the Hankel integral transformation methods, while equality of the rotary angle of the pile axis and z-axis of the porous medium is used as the compatibility condition between the pile and the porous medium. Based on the researches of the present paper, the following conclusion can be drawn.

[1] The analysis and numerical calculation of the paper shows that Fredholm integral equation and fictitious pile methodology can be used in the investigation of a pile embedded in a porous medium and subjected to plane seismic waves. Our calculation shows a considerable difference on the pile response between the single phase model and the porous medium model. Consequently, for saturated soil, rock or sand, to achieve more reasonable results, it is better option to use the saturated porous medium model.

[2] Numerical results show that the permeability of the porous medium, the modulus ratio between the pile and the porous medium and the frequency of the incident wave all have a direct influence on the dynamic response of the pile. Generally, lower frequency seismic waves tend to generate larger displacement and smaller shear force and pore pressure, while higher frequency seismic waves tend to generate smaller displacement. In our examples, the largest shear force and pore pressure are produced by an incident wave with 100 Hz frequency.

[3] The presented methodology can be extended to calculate the time domain response of piles embedded in a porous medium and subjected to SH waves. Using the superposition principle, pile group problems can also be solved by the proposed approach. The scattering of P and SV or Rayleigh waves by a pile or pile group embedded in a porous medium can also be resolved by the suggested approach.

Acknowledgments: The project is supported by National Natural Science Foundation of China with grant number No. 50578071. The authors are grateful for the help of Miss Sally Williams at USYD in editing this paper.

References

Achenbach JD. (1973) *Wave propagation in elastic solids*. North-Holland, Amsterdam.

Biot MA.(1941) General theory of three-dimensional consolidation. *Journal of Applied Physics*, 12: 155-164.

Biot (1956a) MA. Theory of propagation of elastic waves in a fluid-saturated porous solid, I, Low frenquency range. *Journal of the Acoustical Society of America*, 28: 168-178.

Biot MA. (1956b) Theory of propagation of elastic waves in a fluid-saturated porous solid, II: Higher frequency range. *Journal of the Acoustical Society of America*, 28: 179-191.

Biot MA and Willis DG. (1957) The elastic coefficients of the theory of consolidation. *Journal of Applied Mechanics*, 24: 594–601.

Biot MA. (1962) Mechanics of deformation and acoustic propagation in porous media. *Journal of Applied Physics*, 33: 1482-1498.

Berrill J, Yasuda S. (2002) Liquefaction and piled foundations: Some issues. *Journal of Earthquake Engineering*, 6: 1-41.

Bonnet G. (1987) Basic singular solutions for poroelastic medium in the dynamic range. *Journal of the Acoustical Society of America*, 82:,1758–1762.

Boonsrang N, Pisidhi K. (1981) Load transfer from an elastic pile to a saturated porous elastic soil. *International journal for numerical and analytical methods in Geomechanics*, 5:115-138.

Broms BB. (1964). Lateral resistance of piles in cohesive soils. *Journal of the Soil Mechanics and Foundations Division ASCE* 1964; 90(SM2):27-63.

Butterfield R and Banerjee PK. (1971). The elastic analysis of compressible piles and pile groups. *Geotechnique*, 21: 43-60.

Eason G. The stresses produced in a semi-infinite solid by a moving surface force. Int. J. Engng. Sci. 1965, 2: 581-609.

Fan K, Gazetas G, Kaynia A, et al. (1991) Kinematic seismic response of single piles and pile groups. *Journal of Geotechnical Engineering-ASCE*, 117: 1860-1879.

Gassmann F. (1951). Über die Elastizität poröser Medien. Vier. *der Natur. Gesellschaft in Zürich*, 96: 1–23.

Halpern MR and Christiano P. (1986) Steady-state harmonic response of a rigid plate bearing on a liquid-saturated poroelastic halfspace. *Earthquake Engineering and Structural Dynamics*, 14: 439–454.

Johnson DL, Koplik J, Dashen R. (1987) Theory of dynamic permeability and tortuosity in fluid-saturated porous-media. *Journal of Fluid Mechanics*, 176: 379-402.

Karkee MB, Kishida H. (1997). Investigations on a new building with pile foundation damaged by the Hyogoken-Nambu (Kobe) earthquake. *Structural Design of Tall Buildings*, 311-332.

Lu JF. (2000) *The Interaction between Piles and Saturated Soil*. PHD Dissertation of Shanghai Jiao-Tong University. Shanghai, China.

Lu, JF. (2002) Frequency domain dynamic analysis of laterally loaded piles embedded in saturated half-space. *Chinese Journal of Rock Mechanics and Engineering*, 21: 577-581.

Luco JE and Apsel RJ. (1983). On the Green's functions for a layered half-space: Part I. *Bull Seism Soc Am*, 73: 909-929.

Mamoon SM and Banerjee PK. (1990) Response of piles and pile groups to traveling SH-waves. *Earthquake Engineering & Structural Dynamics*, 1990; 19: 597-610.

Muki R. (1960) Asymmetric problem of the theory of elasticity for a semi-infinite solid and a thick plate. *Progress in Solid Mechanics* 1 (Edited by Sneddon IN and Hill R). Amaterdam North Holland, Interscience, New York, 399.

Muki R and Sternberg E. (1970) Elastostatic load-transfer to a half-space from a partially embedded axially loaded rod. *International Journal of Solids and Structures* 1970; 6: 69-90.

Pak RY and Jennings PC. (1987) Elasticdynamic response of pile under transverse excitations. *Journal of Engineering Mechanics Division, ASCE*, 113:1101-1116.

Poulos HG and Davis EH. (1980) *Pile Foundation Analysis and Design*, John Wiley and Sons, 1980.

Pride SR, Morgan FD and Gangi AF. (1993) Drag forces of porous-medium acoustics. *Physical Review B*, 47: 4964-4978.

Sen R, Davies TG and Banerjee PK. (1985) Dynamic analysis of piles and pile groups embedded in homogeneous soils. *Earthquake Engineering & Structural Dynamics*, 13: 53-65.

Sneddon IN. (1951) *Fourier transforms*. New York, NY: McGraw-Hill; 1951.

Takemiya H and Yamada Y. (1981) Layered soil-pile-structure dynamic interaction. *Earthquake Engineering & Structural Dynamics*, 9: 437-457.

Tokimatsu K, amd Suzuki H. (2004) Pore water pressure response around pile and its effects on P-Y behavior during soil liquefaction. *Soils and Foundations*, 44: 101-110.

Wang JH, Zhou XL, and Lu JF. (2003) Dynamic response of pile groups embedded in a poroelastic medium. *Soil Dynamics and Earthquake Engineering*, 23: 235-242.

Youd TL and Bartlett SF. (1989) Case histories of lateral spreads from the 1964 Alaskan earthquake, *Proceedings, Third Japan-U.S. Workshop on Earthquake Resistant Design of Lifeline Facilities and Countermeasures for Soil Liquefaction*, Report NCEER-91-0001, National Center for Earthquake Engineering Research, SUNY, Buffalo, NY.

Zeng X and Rajapakse RKND. (1999).Dynamic axial load transfer from elastic bar to poroelastic medium. *Journal of Engineering Mechanics-ASCE*, 125: 1048-1055.

Zimmerman C and Stern M. (1993) Boundary element solution of 3-D wave scatter problems in a poroelastic medium. *Engineering Analysis with Boundary Elements*, 12: 223-240.